

AD-A054 316

PURDUE UNIV LAFAYETTE IN TURNER LAB FOR ELECTROCERAMICS F/G 20/12  
THE EFFECTS OF SUBSTRATE COMPOSITION ON THICK FILM CIRCUIT RELI--ETC(U)  
FEB 78 R W VEST

UNCLASSIFIED

N00019-77-C-0327  
NL

[OF]  
AD  
A054316



END  
DATE  
FILMED  
6 -78  
DDC

AD A 054316



FOR FURTHER TRAN ~~SMITH~~  
*See PR045085*

94  
**13**

APPROVED FOR PUBLIC RELEASE  
DISTRIBUTION UNLIMITED

PURDUE UNIVERSITY  
West Lafayette, Indiana



AD No. \_\_\_\_\_  
DDC FILE COPY

SCHOOL OF MATERIALS ENGINEERING

*J* DDC  
RECEIVED  
MAY 26 1978  
D

AD A 054316

13

AD NO.  DDC FILE COPY

THE EFFECTS OF SUBSTRATE COMPOSITION  
ON THICK FILM CIRCUIT RELIABILITY

R. W. Vest

28 February 1978

Final Technical Report

For the period 2/1/77 - 1/31/78

Contract No. N00019-77-C-0327

Prepared for

NAVAL AIR SYSTEMS COMMAND

DDC  
RECEIVED  
MAY 26 1978  
D

**DISTRIBUTION STATEMENT A**

Approved for public release;  
Distribution Unlimited

9 Final rept. 1 Feb 77-31 Jan 78

SECURITY CLASSIFICATION OF THIS PAGE (When Data Entered)

REPORT DOCUMENTATION PAGE		READ INSTRUCTIONS BEFORE COMPLETING FORM
1. REPORT NUMBER	2. GOVT ACCESSION NO.	3. RECIPIENT'S CATALOG NUMBER
4. TITLE (and Subtitle) 6 THE EFFECTS OF SUBSTRATE COMPOSITION ON THICK FILM CIRCUIT RELIABILITY.		5. TYPE OF REPORT & PERIOD COVERED Final Report (2/1/77 to 1/31/78)
		6. PERFORMING ORG. REPORT NUMBER
7. AUTHOR(s) 10 R. W./Vest		8. CONTRACT OR GRANT NUMBER(s) 15 N00019-77-C-0327
9. PERFORMING ORGANIZATION NAME AND ADDRESS Purdue Research Foundation, Purdue University West Lafayette, Indiana 47907		10. PROGRAM ELEMENT, PROJECT, TASK AREA & WORK UNIT NUMBERS
11. CONTROLLING OFFICE NAME AND ADDRESS Naval Air Systems Command Washington, DC 20361		12. REPORT DATE 28 Feb 1978
		13. NUMBER OF PAGES
14. MONITORING AGENCY NAME & ADDRESS (if different from Controlling Office)		15. SECURITY CLASS. (of this report) Unclassified 12/68p
		15a. DECLASSIFICATION/DOWNGRADING SCHEDULE N/A
16. DISTRIBUTION STATEMENT (of this Report)  <b>APPROVED FOR PUBLIC RELEASE: DISTRIBUTION UNLIMITED</b>		
17. DISTRIBUTION STATEMENT (of the abstract entered in Block 20, if different from Report)		
18. SUPPLEMENTARY NOTES		
19. KEY WORDS (Continue on reverse side if necessary and identify by block number) Thick film resistors      Temperature coefficient resistivity Ceramic substrates      Electronic glass Electrical resistivity		
20. ABSTRACT (Continue on reverse side if necessary and identify by block number) Studies of the rate of dissolution of 96% Al <sub>2</sub> O <sub>3</sub> substrates (AlSiMag 614) in a model glass (63 w/o PbO-20 w/o B <sub>2</sub> O <sub>3</sub> -10 w/o SiO <sub>2</sub> ) were conducted as a function of temperature from 750° to 950°C. The rate limiting step was found to be molecular diffusion of substrate ingredients in the glass at times pertinent to thick film processing. Data from experiments on substrate dissolution in glasses having varying amounts of substrate previously dissolved were utilized to develop an analytical expression which will give the		

DD FORM 1 JAN 73 1473

EDITION OF 1 NOV 65 IS OBSOLETE  
S/N 0102-014-6601

SECURITY CLASSIFICATION OF THIS PAGE (When Data Entered)

410 421 Gu

substrate recession as a function of time and temperature for an actual thick film resistor; predictions of this equation compared favorably with experimental data. Studies of the initial stages of glass sintering as a function of temperature and the amount of substrate dissolved in the glass were utilized to develop an analytical expression for the surface tension to viscosity ratio of the glass as a function of temperature and the amount of substrate dissolved. Studies of the influence of substrate constituents dissolved in the glass on the electrical properties of resistors showed a significant effect on both sheet resistance and temperature coefficient of resistance (TCR). The sheet resistance increased and the TCR decreased as the amount of substrate dissolved in the glass increased for the same processing conditions. These results are consistent with the present model of charge transport processes in thick film resistors.

FORWARD

Research described in this report constitutes the second year of effort under a contract with the Naval Air Systems Command, Department of the Navy, under the technical cognizance of James Willis. The research was conducted in the Turner Laboratory for Electroceramics, School of Materials Engineering and School of Electrical Engineering, Purdue University, West Lafayette, Indiana 47907, under the direction of Professor R. W. Vest. Contributing to the Project were G. L. Fuller, J. M. Himelick, P. Palanisamy, R. L. Reed and D. Tandan.

ACCESSION for		
DTIC	White Section	<input checked="" type="checkbox"/>
DDC	Buff Section	<input type="checkbox"/>
UNANNOUNCED		<input type="checkbox"/>
JUSTIFICATION.....		
BY.....		
DISTRIBUTION/AVAILABILITY CODES		
GEN.	AVAIL.	and/or SPECIAL
A		

## TABLE OF CONTENTS

Section	Page
I. INTRODUCTION . . . . .	.1
II. RESISTOR - SUBSTRATE INTERACTION KINETICS. . . . .	.5
A. Review of Theory and Prior Work. . . . .	.5
B. Experimental procedure . . . . .	.7
C. Results and Analysis . . . . .	.9
D. Discussion . . . . .	14
III. GLASS SINTERING STUDIES . . . . .	22
A. Review of Theory and Prior Work. . . . .	22
B. Experimental Procedure . . . . .	24
C. Results and Analysis . . . . .	25
D. Discussion . . . . .	40
IV. ELECTRICAL EFFECTS . . . . .	42
A. Experimental Procedure . . . . .	42
B. Results and Analysis . . . . .	47
C. Discussion . . . . .	54
V. FUTURE PLANS . . . . .	55
VI. REFERENCES . . . . .	56
APPENDIX . . . . .	58
A. Glass Preparation . . . . .	58
DISTRIBUTION LIST . . . . .	61

## LIST OF FIGURES

Figure		Page
II.1	Dissolution of AlSiMag 614 Substrate in 63-25-12 Glass . . . .	10
II.2	Dissolution of AlSiMag 614 Substrate in 63-25-12 Glass - Short times . . . . .	11
II.3	Dissolution of AlSiMag 614 Substrate in 63-25-12 Glass with 5w/o AlSiMag 614. . . . .	12
II.4	Dissolution of AlSiMag 614 Substrate in 63-25-12 Glass with 10w/o AlSiMag 614 . . . . .	13
II.5	Dependence of AlSiMag 614 Dissolution Rate on Temperature and Glass Composition . . . . .	15
II.6	Recession of AlSiMag 614 Substrates under Printed and Fired 5w/o RuO <sub>2</sub> Resistors. . . . .	16
II.7	Comparison of Eq. II.5 with Experiment for Substrate Recession Rate Dependence on Glass Composition . . . . .	18
II.8	Comparison of Theory and Experiment for Dissolution of AlSiMag 614 in Thick Film Resistors . . . . .	21
III.1	Initial Stage of Viscous Flow Sintering . . . . .	23
III.2	Initial Stage Sintering of 63-25-12 Glass Spheres at 503°C . .	26
III.3	Initial Stage Sintering Kinetics for Standard 63-25-12 Glass .	27
III.4	Initial Stage Sintering Kinetics for 0-I 63-25-12 Glass. . . .	28
III.5	Initial Stage Sintering Kinetics for Standard 70-20-10 Glass .	29
III.6	Surface Tension to Viscosity Ratio for Base Glass Compositions.	31
III.7	Initial Stage Sintering Kinetics for 63-2F-12 Glass in Dry Air	33
III.8	Effect of Relative Humidity on Surface Tension to Viscosity Ratio of 63-25-12 Glass. . . . .	35
III.9	Initial Stage Sintering Kinetics for 63-25-12 Glass with 2w/o AlSiMag 614 in Dry Air . . . . .	36
III.10	Initial Stage Sintering Kinetics for 63-25-12 Glass with 6w/o AlSiMag 614 in Dry Air . . . . .	37
III.11	Initial Stage Sintering Kinetics for 63-25-12 Glass with 10w/o AlSiMag 614 in Dry Air. . . . .	38
III.12	Effect of Dissolved AlSiMag 614 on Surface Tension to Viscosity Ratio of 63-25-12 Glass. . . . .	39
IV.1	Effect of 8w/o AlSiMag 614 in 70-20-10 Glass on 5w/o RuO <sub>2</sub> Resistors Sintered on Glazed Platinum Substrates - TCR <sup>2</sup> . . .	48

LIST OF FIGURES CONTINUED

	Page
IV.2 Effect of 10w/o AlSiMag 614 in 63-25-12 Glass on 5w/o RuO <sub>2</sub> Resistors Sintered on AlSiMag 614 Substrates-Sheet Resistance and VCR . . . . .	.50
IV.3 Effect of 10w/o AlSiMag 614 in 63-25-12 Glass on 5w/o RuO <sub>2</sub> Resistors Sintered on AlSiMag 614 Substrate - TCR. . . . .	.51
IV.4 Effect of 10w/o AlSiMag 614 in 63-25-12 Glass on Non-supported 5w/o RuO <sub>2</sub> Resistors - TCR. . . . .	.53
A.1 Glass Melting Furnace. . . . .	.59

## I. INTRODUCTION

The ceramic substrate upon which thick film circuits are printed and fired is a carrier for the circuit, but it is also a source of reactive material. It has been shown that the sheet resistance, temperature coefficient of resistance, and noise index of thick film resistors are affected by the substrate [1]. Studies have also demonstrated that the adhesion of conductives and the thermal degradation of the adhesion are functions of the choice of substrate material [2].

The print and fire processing of thick film circuits ensures that there will always be some degree of chemical interaction between the film and the substrate, because all common substrate materials are soluble to some degree in the glass used in thick film inks. This interaction is primarily responsible for the development of adhesion between the thick film resistor and the substrate. By virtue of the resistor-substrate interaction, the composition of the glass is changed, and as a consequence all of the physical properties of the glass will change to some extent. These changes in physical properties of the glass will result in modified kinetics for the various microstructure development processes in thick film resistors, and all electrical properties of the resistors are related to their microstructure.

The goal of this research program is to develop a sufficient level of understanding of the phenomena involved so that appropriate models can be developed. These models should lead to the writing of specifications for impurity limits and additive ranges for substrates, and to recommendations concerning glass composition and processing conditions.

One influence of the substrate on microstructure development in thick film resistors was demonstrated during an earlier project at Purdue [3]

involving X-ray diffraction line broadening experiments designed to study the growth of  $\text{RuO}_2$  conductive particles in the resistor. Test resistors prepared in the normal way by screen printing the formulation on 96%  $\text{Al}_2\text{O}_3$  substrates showed a much slower growth rate of  $\text{RuO}_2$  than samples prepared by mixing the  $\text{RuO}_2$  and glass powders in the same proportions as in the formulation and heating this mixture in a platinum crucible. The presence of the substrate appeared to buffer the crystallite size after an initial rapid increase. X-ray phase analysis results did not indicate any new crystalline phases formed due to interactions between any of the ingredients ( $\text{RuO}_2$ -glass-substrate) for the time-temperature conditions employed in the ripening studies, but it was found that alumina was readily soluble in the glass. Contact angle measurements using glass with ten weight percent substrate material dissolved in it showed complete wetting to  $\text{RuO}_2$ , but the rate of spreading was much slower than for the normal glass. The glass would penetrate the  $\text{RuO}_2$  particles at a slower rate and the driving forces responsible for the early stages of microstructure development would be displaced to higher temperatures; however, these temperatures are still well below the temperature range of the ripening studies. In order to determine the change in the viscosity and surface tension of the glass due to dissolution of the substrate, shrinkage measurements were conducted on compacts of glass powder with and without substrate material dissolved in it. The time dependence of the linear shrinkage of a compact consisting of spherical particles undergoing initial stage sintering by Newtonian viscous flow is directly proportional to time, and the proportionality constant contains the ratio of the surface tension to the viscosity. The surface tension to viscosity ratio for the glass with ten weight percent substrate dissolved was only one-fourth that of the normal glass, but this change was not nearly large enough to account for

the observed change in ripening kinetics. Since the results of neither the contact angle nor the viscosity-surface tension measurements using the glass with ten weight percent substrate material dissolved could explain the observed effect of substrate-resistor interactions, it was believed that these interactions changed the composition of the glass such that the solubility of  $\text{RuO}_2$  in the glass was reduced. Reduction in the solubility of  $\text{RuO}_2$  in the glass further reduces the phase boundary reaction controlled solution-precipitation process and hence the rate of growth of  $\text{RuO}_2$  particles.

Another role played by the glass in thick film resistors is that of a charge transport medium for a certain fraction of the total current carried by the resistor [3]. In addition to well sintered contacts in the conducting network, certain contacts between oxide particles contain a thin glass film and transport through this film is an important part of the overall charge transport mechanism. It is suspected that properties such as voltage coefficient of resistance, temperature coefficient of resistance and current noise are very sensitively related to the number and the characteristics of these contacts. Electrical behavior of such contacts is very strongly related to the impurity content of the glass and hence would be expected to be sensitive to substrate-resistor interactions.

Previously reported studies [4] under this program have shown that the rate of dissolution of 96%  $\text{Al}_2\text{O}_3$  substrates (AlSiMag 614) in a lead borosilicate glass (70w/o  $\text{PbO}$  - 20w/o  $\text{B}_2\text{O}_3$  - 10w/o  $\text{SiO}_2$ ) was limited by the phase boundary reaction at times important to thick film resistor processing. Rate equations were developed to allow the prediction of the total quantity of substrate dissolved in the resistor glass under any processing conditions. Standard processing (800°C, 10 minutes) will result in a fired resistor volume containing up to 20% of ingredients

derived from the substrate. Studies of the distribution of the substrate ingredients throughout the resistor glass at 800°C produced results consistent with a step change in concentration at the substrate-resistor interface. Dissolution rate studies with 99.5%  $\text{Al}_2\text{O}_3$  substrates (AlSiMag 772) showed similar results and were consistent with the proposed rate limiting step. The presence of substrate constituents dissolved in the glass were shown to have a significant effect on the temperature coefficient of resistance (TCR) of  $\text{RuO}_2$  - glass composites. A low TCR characteristic of reliable thick film resistors cannot be achieved with the model system unless an appreciable amount of substrate materials is dissolved in the resistor glass.

The conductive component of all thick film resistors studied during this year was ruthenium dioxide ( $\text{RuO}_2$ ), and the substrate was AlSiMag 614 (96%  $\text{Al}_2\text{O}_3$ ). Two base glass compositions were studied; 63w/o  $\text{PbO}$  - 25w/o  $\text{B}_2\text{O}_3$  - 12w/o  $\text{SiO}_2$  and 70w/o  $\text{PbO}$  - 20w/o  $\text{B}_2\text{O}_3$  - 10w/o  $\text{SiO}_2$ . The characterization of these ingredient materials was presented in a previous report [4], and the techniques and equipment for preparation of the glasses are described in the Appendix.

## II. RESISTOR - SUBSTRATE INTERACTION KINETICS

### A. REVIEW OF THEORY AND PRIOR WORK

There are several possible rate limiting steps for dissolution of an alumina substrate in a thick film resistor glass. At relatively short times the dissolution rate may be controlled by the chemical reaction rate at the glass-substrate interface [5]. As the concentration of solute near the interface increases it is necessary to remove the substrate material in solution from the interface region in order for the reaction to continue. In the absence of flow producing hydrostatic instabilities the mass transport will be limited by molecular diffusion in the glass [6]. At longer times a boundary layer is built up between the interface and the bulk glass, and due to temperature, density or surface tension gradients in the boundary area the region becomes hydrostatically unstable resulting in a substrate recession rate governed by natural convection [7]. The width of the boundary layer will change if a source of forced convection exists; for example, a solution for mass transfer from rotating discs has been derived [8] and verified experimentally [9]. These various mechanisms have been discussed in the previous annual report [4] on this project and are summarized in Table II.I.

A considerable amount of work has been published for both single crystal and polycrystalline alumina dissolution in various glass melts under conditions of both free and forced convection [5, 7, 10-15]; these references were discussed in the previous annual report [4]. Previous studies [4] of the dissolution of both AlSiMag 614 and AlSiMag 772 substrates in 70-20-10 glass indicated a linear dependence of substrate recession ( $Y$ ) on time. Both substrates showed a change to a smaller, but still constant, recession rate after some time  $t_c$ , but the time-temperature

TABLE II.1

## SUBSTRATE DISSOLUTION: MECHANISMS

MECHANISM	RATE EQUATION	PRIMARY ASSUMPTIONS
Interface Reaction	$Y = K \frac{A_C}{A_0} t$	a. $A_C$ and $K$ are time independent b. infinite glass reservoir
Molecular Diffusion	$Y = 2 \alpha \sqrt{D^* t}$	a. semi-infinite slab b. infinite glass reservoir
Boundary Layer Diffusion	$Y = \frac{DC^*}{\delta} t$	a. natural convection b. infinite glass reservoir c. infinite slab
Boundary Layer Diffusion	$Y = 0.61 D^{2/3} C^* \nu^{-1/6} \omega^{1/2} t$	a. forced convection b. infinite glass reservoir c. rotating disc
K = reaction rate constant $A_C$ = actual interface area $A_0$ = geometric interface area $\alpha$ = a constant $D^*$ = effective binary diffusion coefficient		D = diffusion coefficient in the boundary layer $C^*$ = a concentration parameter $\delta$ = boundary layer thickness $\nu$ = effective kinematic viscosity of boundary layer $\omega$ = angular velocity of rotating disc

relationships important in thick film processing lie within the first segment. Studies of the diffusion of substrate ingredients into the glass indicated a step function change in concentration at the interface and a constant concentration of substrate ingredients throughout the glass. This means that the diffusion of substrate ingredients away from the interface region must be fast in comparison with the movement of atoms across the interface, thereby favoring the reaction rate limiting mechanism. The differences observed between the behavior of AlSiMag 614 and AlSiMag 772 substrates were explained on the basis of preferred orientation of corundum crystals. The 772 substrates have been shown [16] to favor grains with the basal plane (0001) parallel to the substrate surface, which would lead to a slower dissolution rate based on previous results with sapphire crystals [4, 16].

Two types of experiments were conducted under the present study. In the first set of experiments the solubility of AlSiMag 614 substrates in bulk 63-25-12 glass and in bulk 63-25-12 glass containing varying amounts of dissolved substrate was measured as a function of time and temperature. In the second set of experiments the solubility of AlSiMag 614 substrates in printed and fired thick film resistors was measured.

#### B. EXPERIMENTAL PROCEDURE

For the bulk glass experiments, the glass was raised to the desired temperature in a platinum crucible and a clean, 2.5 cm square substrate held in a platinum wire harness was suspended immediately above it for 3 minutes to allow for thermal equilibrium. The substrate was then immersed in the glass for the required time. At the end of the time period the substrate was removed from the glass, air quenched and placed in concentrated HCl to leach away the adhering glass. During this time the chip was given 3 hours of ultrasonic agitation to aid in the glass

decomposition and then allowed to stand until all glass was removed. The chip was then rinsed in water followed by acetone, dried, weighted, and the recession of the substrate surface calculated from the equation:

$$\gamma = \frac{b - (b^2 - 4ac)^{1/2}}{2a} \quad (\text{II.1})$$

where

$$a = 4(\rho d_0 / W_0)^{1/2}$$

$$b = 1 + d_0 a / 2$$

$$c = d_0 (W_0 - W_t) / 2W_0$$

$\rho$  = substrate density

$d_0$  = substrate initial thickness

$W_0$  = substrate initial weight

$W_t$  = substrate final weight

This equation was derived in the previous annual report [4].

Two sets of control experiments were conducted to determine the degree of attack of the substrate alone by HCl and to assure that all the glass was removed from the substrate when following the procedure. Four substrates which had never been exposed to glass were taken through the acid leach process; the average weight change was less than 0.1 mg which was within the accuracy limits of the analytical balance used for these measurements. For the second control, 6 substrates were dipped in the glass for less than 10 seconds at 800°C and then taken through the acid leach process; the average weight loss was less than 0.3 mg indicating that all the glass was removed to the accuracy that weighings could be made.

For studies of substrate dissolution in resistor films, clean, 2.5cm square substrates were screen printed with a resistor formulation containing 5%  $\text{RuO}_2$  relative to 63-25-12 glass. This composition has been shown [3] to produce resistors having a nominal sheet resistance of  $100\text{K}\Omega/\text{square-mil}$ . These resistors were then dried to remove the organic constituents of the formulation, placed in a platinum dish and inserted in a furnace for varying times at different temperatures. The resistor pattern covered an area of  $5.75\text{ cm}^2$ , and the fired resistors were approximately  $25\text{ }\mu\text{m}$  thick. At the end of the time period the resistor was removed from the furnace, air-quenched and carried through the acid leach process described above for the bulk glass experiment. The recession for the substrate surface was then calculated by dividing the weight change by the substrate density and the resistor area.

### C. RESULTS AND ANALYSIS

Results for the surface recession of AlSiMag 614 substrates in bulk 63-25-12 glass at 5 temperatures are shown in Fig. II.1. The recession appears to approach a linear time dependence at sufficiently long times, but the recession rate is more rapid during the initial period at all temperatures. Fig. II.2 shows only the short time portion of Fig. II.1, and  $Y$  is plotted as a function of  $\sqrt{t}$ ; a good linear fit is observed for all 5 temperatures. This is the behavior expected if molecular diffusion of the substrate ingredients in the glass is the rate limiting step (see Table II.I). Similar experiments were performed using glasses which contained 5 w/o and 10 w/o AlSiMag 614 dissolved in them prior to conducting the experiments. The data for substrate recession in these glasses for  $Y$  values below  $14\text{ }\mu\text{m}$  are plotted as a function of  $\sqrt{t}$  in Figs. II.3 and II.4, and a linear fit is obtained with both glasses at

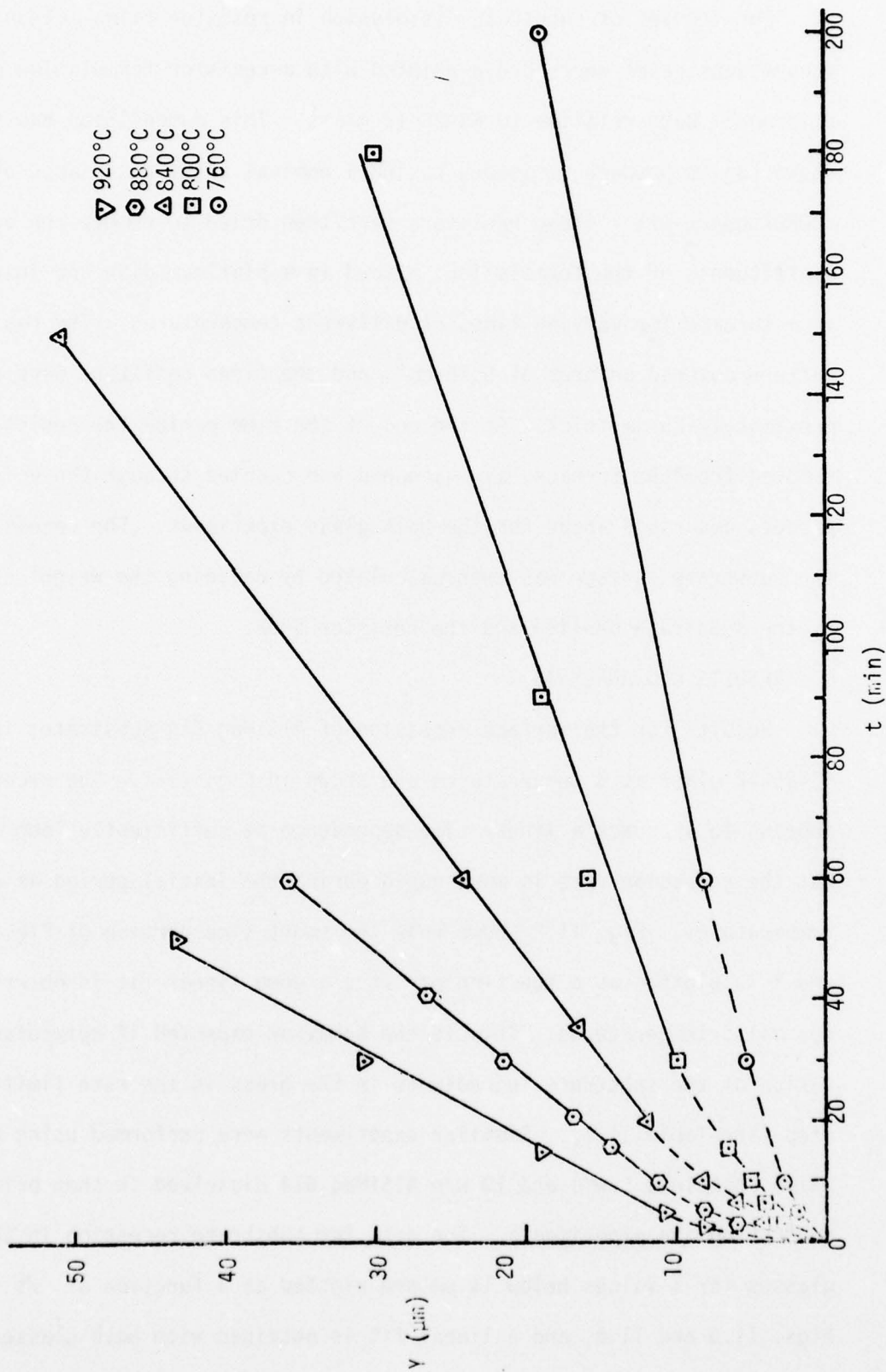


Figure II.1 Dissolution of AlSiMg 614 Substrate in 63-25-12 Glass

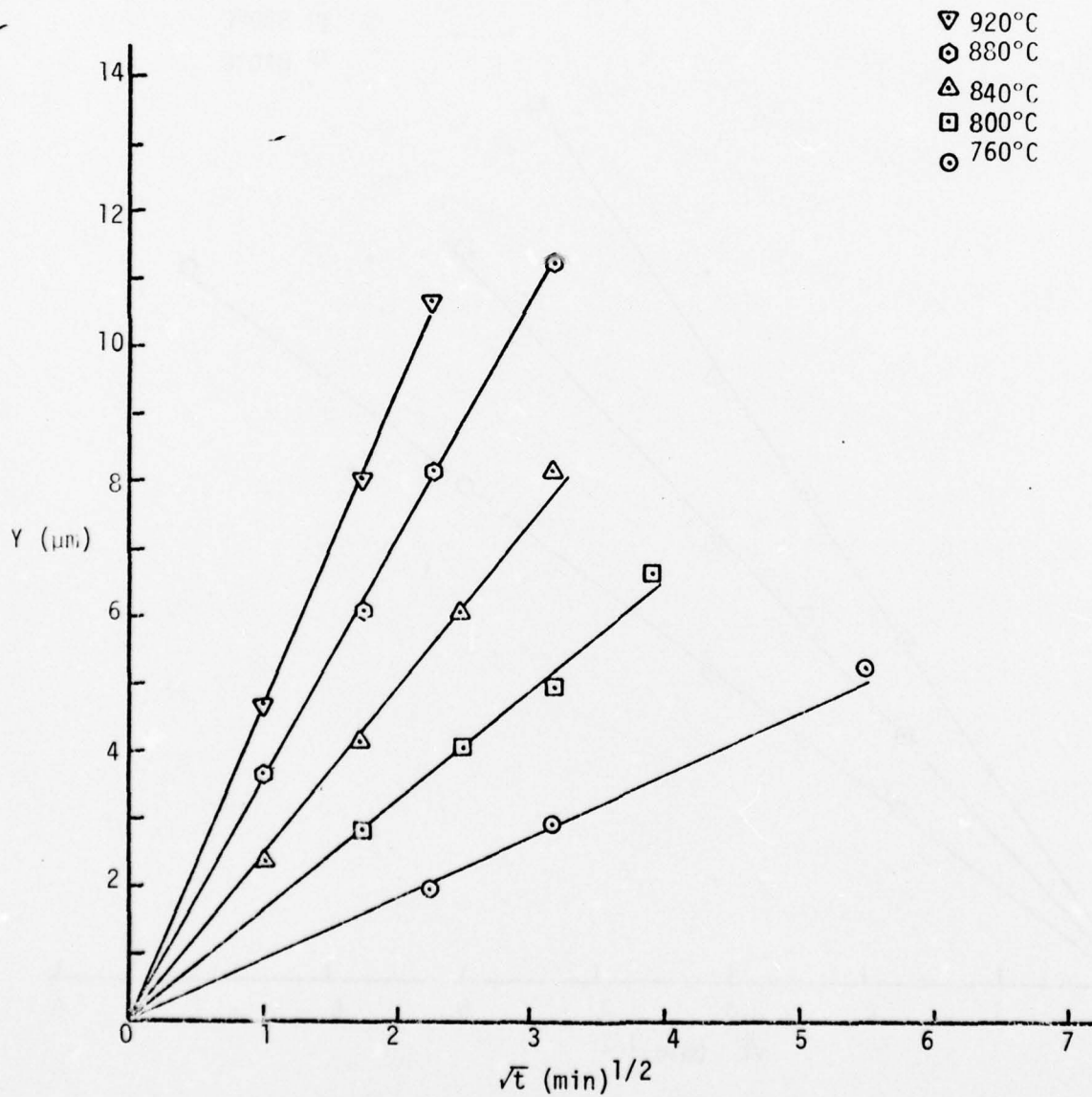


Figure II.2 Dissolution of AlSiMag 614 Substrate in 63-25-12 Glass - Short times

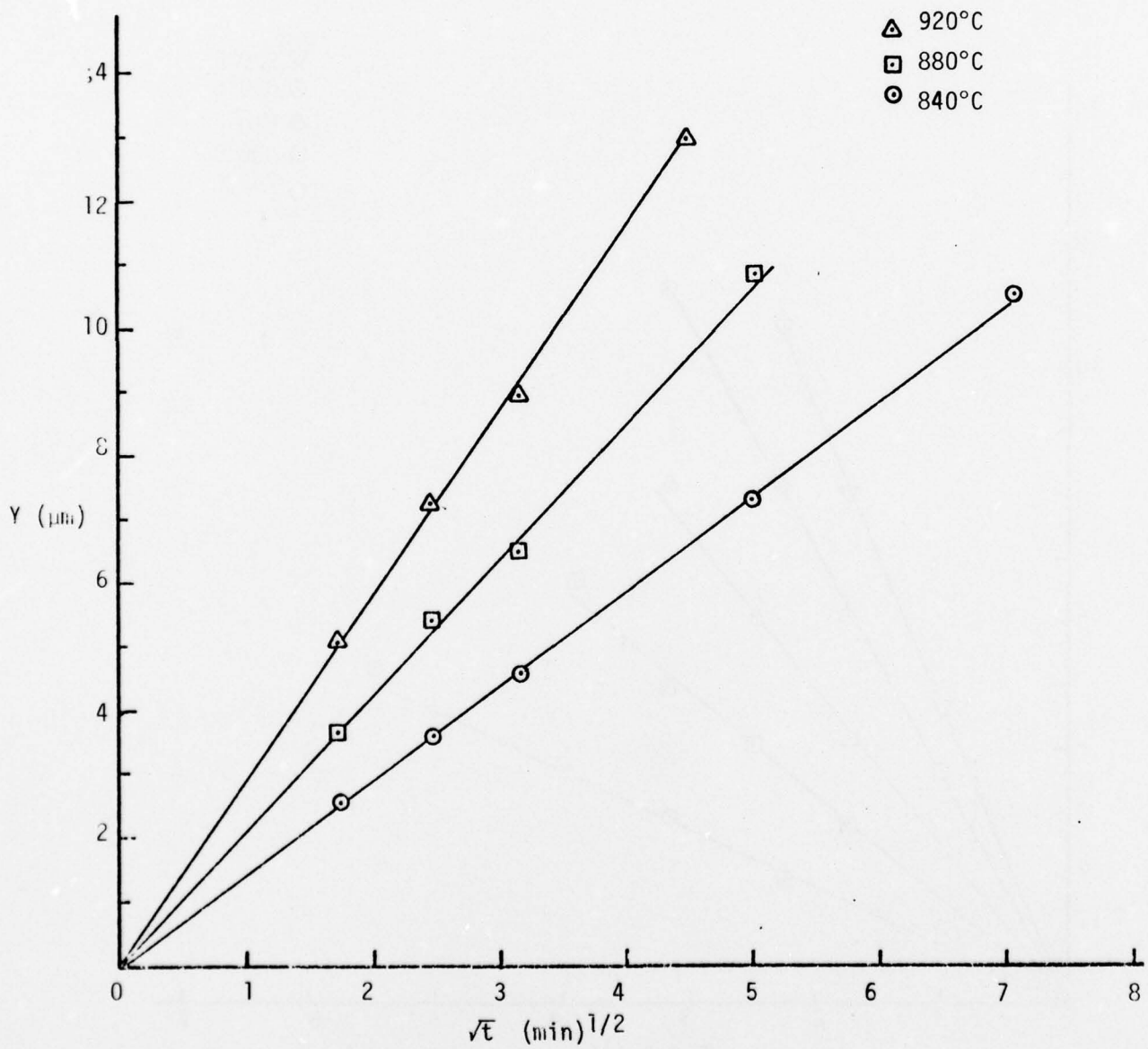


Figure II.3 Dissolution of AlSiMag 614 Substrate in 63-25-12 Glass with 5w/o AlSiMag 614

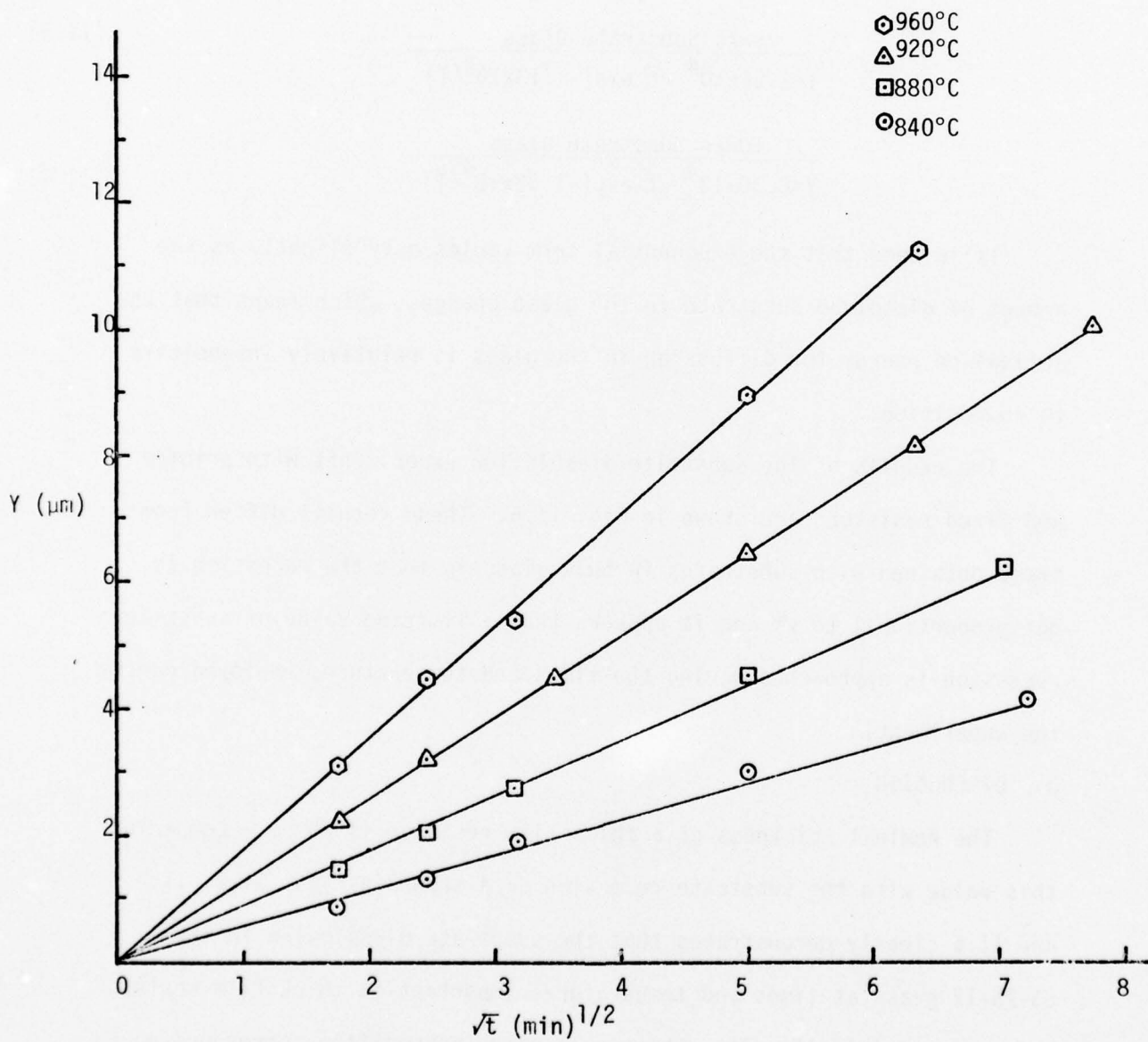


Figure II.4 Dissolution of AlSiMag 614 Substrate in 63-25-12 Glass with 10w/o AlSiMag 614

all temperatures. The slopes of the lines in Figs. II.2 - II.4 were found to be exponentially temperature dependent as shown in Fig. II.5. Least squares analyses of these data resulted in the following relationships.

$$\frac{\text{Base Glass (63-25-12)}}{\gamma = 1.32 \times 10^5 \sqrt{t} \exp(-1.22 \times 10^4 / T)} \quad (\text{II.2})$$

$$\frac{\text{5w/o Substrate Glass}}{\gamma = 3.86 \times 10^4 \sqrt{t} \exp(-1.13 \times 10^4 / T)} \quad (\text{II.3})$$

$$\frac{\text{10w/o Substrate Glass}}{\gamma = 8.30 \times 10^4 \sqrt{t} \exp(-1.32 \times 10^4 / T)} \quad (\text{II.4})$$

It is seen that the exponential term varies only slightly as the amount of dissolved substrate in the glass changes, which means that the activation energy for diffusion in the glass is relatively insensitive to composition.

The results of the substrate dissolution experiments with printed and fired resistors are shown in Fig. II.6. These results differ from those obtained with substrates in bulk glass in that the recession is not proportional to  $\sqrt{t}$  and it appears that a limiting value of substrate recession is approached during the times and temperatures employed during the experiment.

#### D. DISCUSSION

The nominal thickness of a thick film resistor is 25  $\mu\text{m}$ . Comparing this value with the substrate recession data shown in Figs. II.1, II.2 and II.6 clearly demonstrates that the substrate dissolution in the 63-25-12 glass at times and temperatures important in thick film resistor processing is significant. Changes in glass composition corresponding to the substrate recessions shown in Figs. II.1, II.2 and II.6 have significant effects on the properties of the glass and on electrical properties of thick film resistors made from these glasses, as will be discussed in the

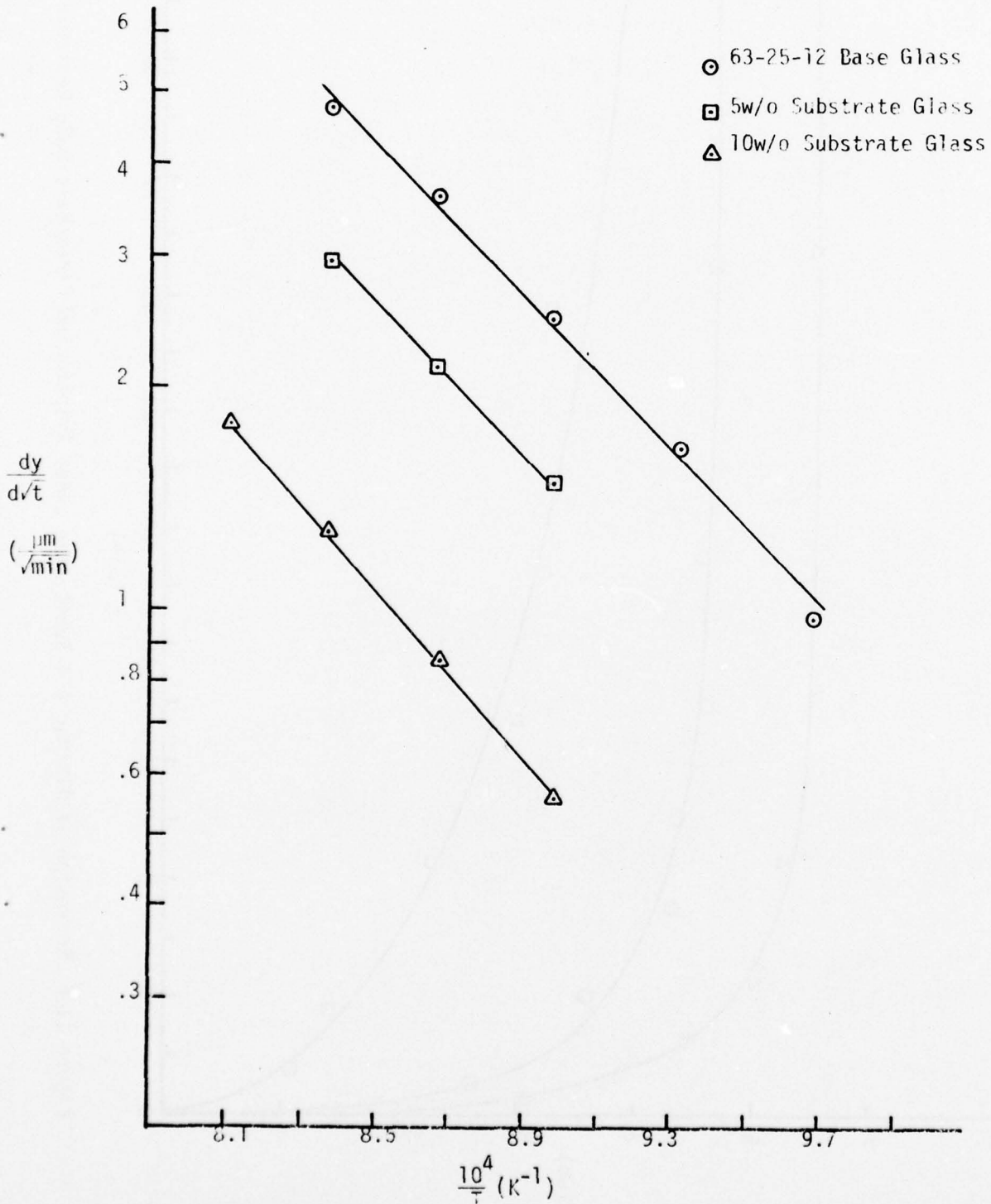


Figure II.5 Dependence of 15SiMag 614 Dissolution Rate on Temperature and Glass Composition.

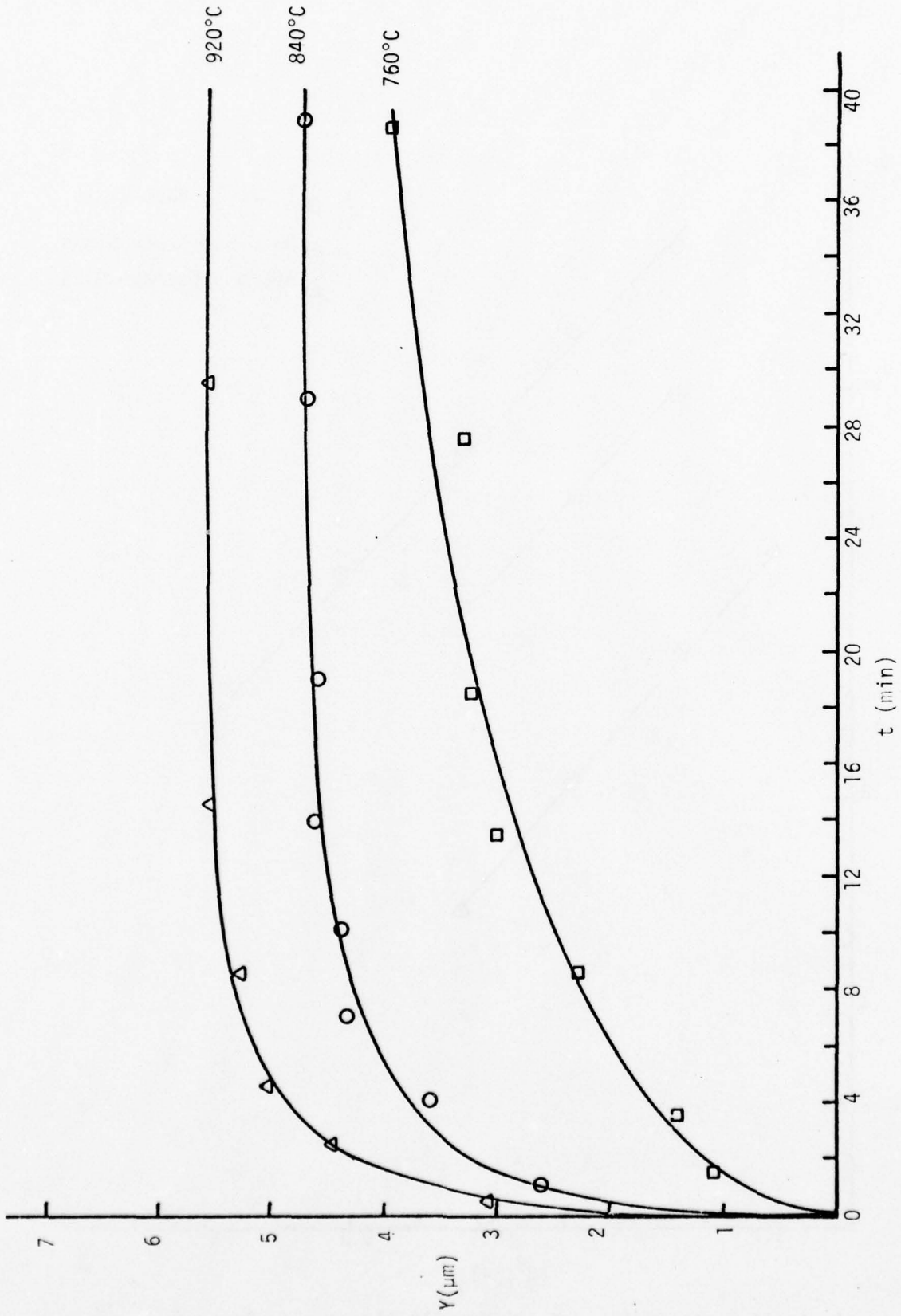


Figure II.6 Recession of AlSiMag 614 Substrates under Printed and Fired 5w/o RuO<sub>2</sub> Resistors

following two sections of this report.

In order to predict the kinetics of the microstructure development processes which control the ultimate electrical properties it is necessary to be able to calculate the composition of the glass for any time and temperature during firing, and the data shown in Fig. II.5 can be utilized to obtain a first order approximation. Equations II.2 - II.4 suggest that there is very little change in the exponential term as the amount of substrate dissolved in the glass changes. Based on this observation, it was assumed that the temperature dependence of the dissolution rate was independent of the amount of substrate dissolved in the glass. Utilizing this assumption, an empirical equation was developed to give the dissolution kinetics as a function of the w/o substrate (P) dissolved in the glass. The data indicated that the dependence of  $dY/d\sqrt{t}$  was almost linear with P, and this linear dependence would predict a zero dissolution rate at approximately 13 w/o dissolved substrate. However, preliminary experiments have shown that the substrate dissolves in glasses having 15 w/o dissolved substrate. Therefore, an empirical expression was developed having a  $P^2$  term in the denominator so that the dissolution rate would decrease rapidly with increasing P, but not go to zero until P was greater than 17 w/o. The empirical equation developed is given below:

$$\frac{dY}{d\sqrt{t}} = \frac{18.1 - 1.02P}{131 + P^2} \times 10^6 \exp(-1.22 \times 10^4/T) \quad (\text{II.5})$$

The excellent fit of Eq. II.5 to the experimental data can be seen in Fig. II.7 for which the lines drawn were calculated from Eq. II.5 and the points are the same experimental points plotted in Fig. II.6.

The experimental data used to generate Eq. II.5 were obtained by measuring the dissolution rate of AlSiMag 614 in an infinite reservoir

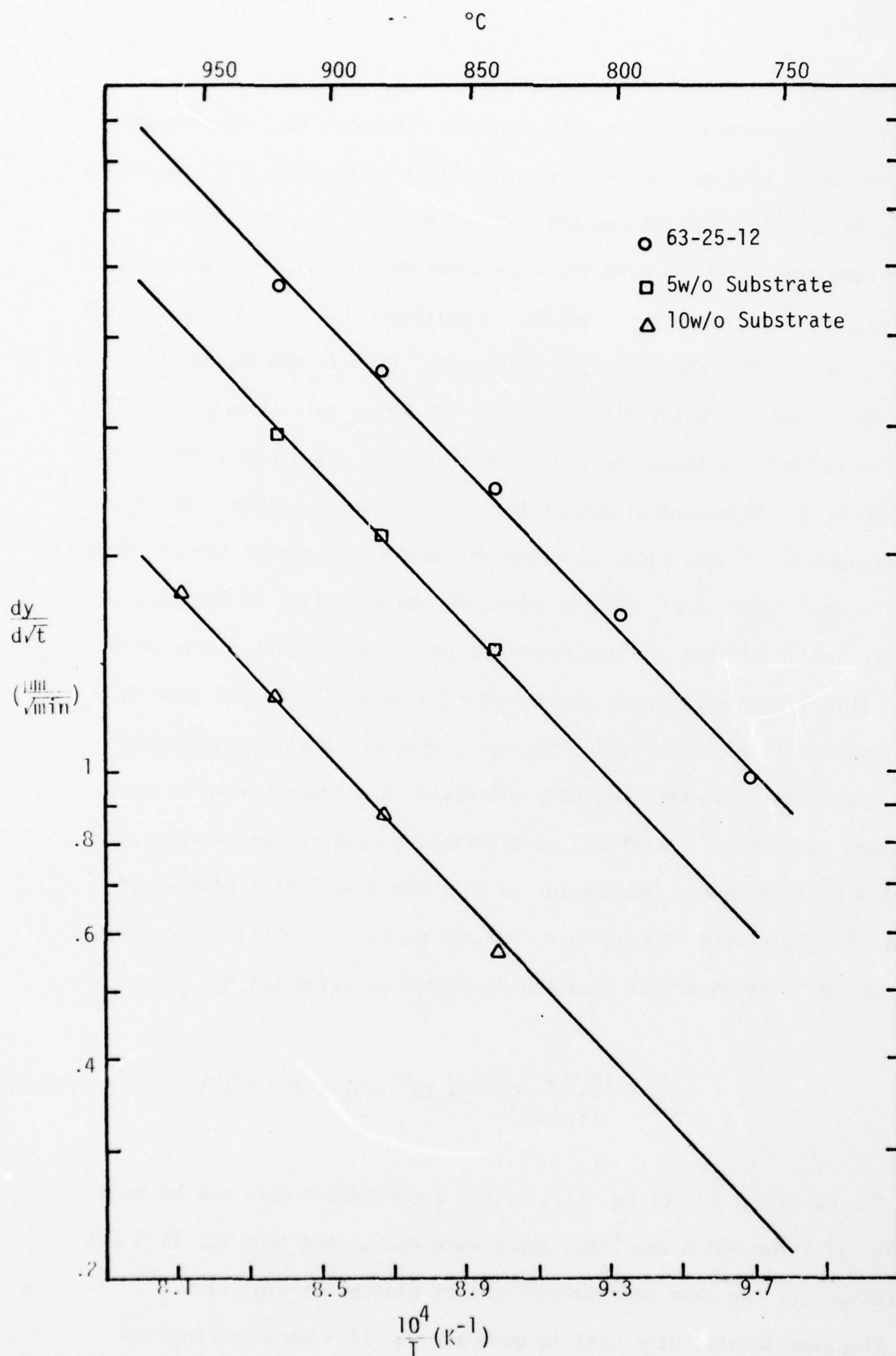


Figure II.7 Comparison of Eq. II.5 with Experiment for Substrate Recession Rate Dependence on Glass Composition

of glass. For the case of a thick film resistor, the glass is not an infinite reservoir relative to the substrate and the glass composition will change as a function of time as the dissolution proceeds. This fact can be accommodated because the volume fraction of substrate ( $V_s$ ) dissolved in a 25  $\mu\text{m}$  thick resistor will be given by:

$$V_s = \frac{Y}{Y+25V_g} \quad (\text{II.6})$$

where  $V_g$  is the volume fraction of glass relative to  $\text{RuO}_2$  in the resistor. Utilizing Eq. II.6 together with the substrate density and the resistor density for a resistor that is 5 w/o  $\text{RuO}_2$  and 95 w/o glass, the following relationship can be developed:

$$P = \frac{100Y}{Y+30.169} \quad (\text{II.7})$$

Substituting Eq. II.7 into Eq. II.5 and rearranging gives:

$$120.8 \int_0^Y \frac{(Y^2+0.7802Y+11.769)dY}{196.4-23.66Y-Y^2} = 10^6 \exp(-1.22 \times 10^4/T) \int_0^t dt^{1/2} \quad (\text{II.8})$$

All intergrals in Eq. II.8 are of standard form and the integration is straightforward, albeit tedious. The integration of Eq. II.8 will give the time required for any degree of substrate recession starting with glass that initially contained no substrate. If some substrate had been dissolved in the glass prior to the resistor firing, this weight percent should simply be added to Eq. II.7 and a new Eq. II.8 calculated and integrated.

Equation II.8 was solved at 760°, 840° and 920°C in order to compare the predictions with the experimental results shown in Fig. II.6 for substrate

dissolution in resistor films. This comparison is shown in Fig. II.8 where the solidlines are those calculated from the integration of Eq. II.8, and the data points are those from Fig. II.6. Reasonably good agreement is obtained between theoretical and experimental points at short times and at long times, but the experimental points lie above the theoretical curves at intermediate times. Part of this discrepancy may be due to an approach to the solubility limit, but another factor may be agitation of the glass by escaping gas bubbles. The theoretical curves are based on data obtained in massive glass where the dissolution mechanism is controlled by the rate of molecular diffusion in the glass. The bubble release, which is known to occur in firing thick film resistors of this composition [3], would provide a stirring action which would be analogous to the forced convection dissolution mechanism discussed in Section IIA. As the firing proceeds, the rate of bubble release decreases and so the discrepancy between the experimental and theoretical curves would be expected to decrease, as is observed.

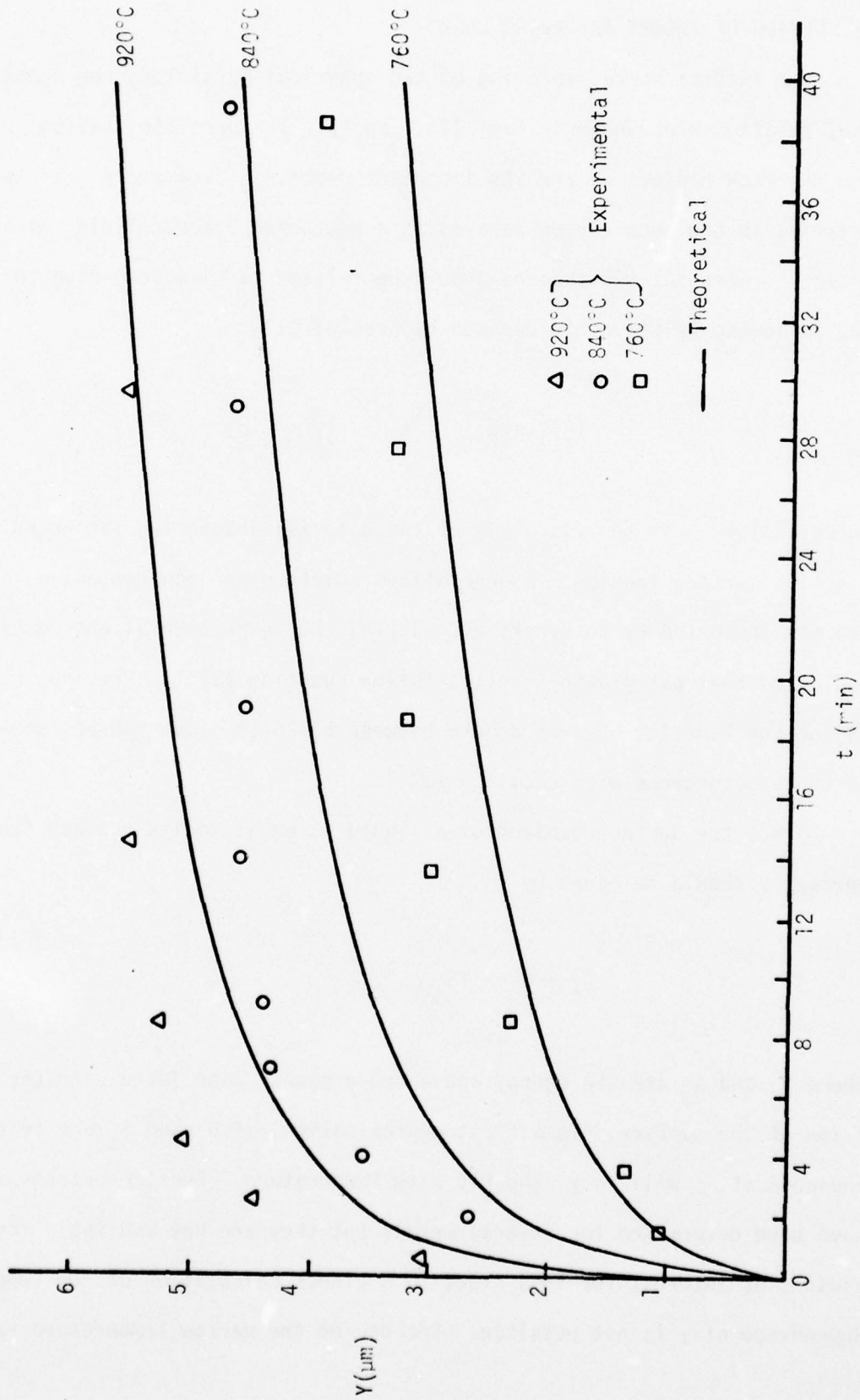


Figure II.8 Comparison of Theory and Experiment for Dissolution of AlSiMag 614 in Thick Film Resistors

### III. GLASS SINTERING STUDIES

#### A. REVIEW OF THEORY AND PRIOR WORK

For initial state sintering of two spherical particles, the geometrical relationships shown in Fig. III.1 apply. The particle radius,  $r$ , and the neck radius,  $x$ , are the important geometric parameters. If the material in the neck region behaves as a Newtonian viscous fluid, neck growth between the two spheres should be related to time according to the following relationship derived by Frenkel [17].

$$\left(\frac{x}{r}\right)^2 = \frac{3}{2} \frac{\gamma}{\eta} r^{-1} t \quad \left(\frac{x}{r} \leq 0.3\right) \quad (\text{III.1})$$

In Eq. III.1,  $\eta$  is the viscosity of the material undergoing sintering and  $\gamma$  is its surface tension. A generalized solution for non-Newtonian fluids has been reported by Kuczynski et. al.[18], but experimental observations indicated that net growth kinetics follow Equation III.1. Previous studies [3] of the kinetics of neck growth between 63-25-12 glass spheres were found to be in accordance with Equation III.1.

Since the surface tension of a liquid is equal to its surface free energy,  $\gamma$  should be given by

$$\gamma = U_s - TS_s \quad (\text{III.2})$$

where  $U_s$  and  $S_s$  are the energy and entropy change associated with the formation of the surface. To a first approximation, if  $U_s$  and  $S_s$  are temperature independent,  $\gamma$  will vary linearly with temperature. Surface entropy values have been determined for several metals but they are not available for the glasses of interest for this study so a direct calculation of the temperature dependence of  $\gamma$  is not possible. Because of the narrow temperature range

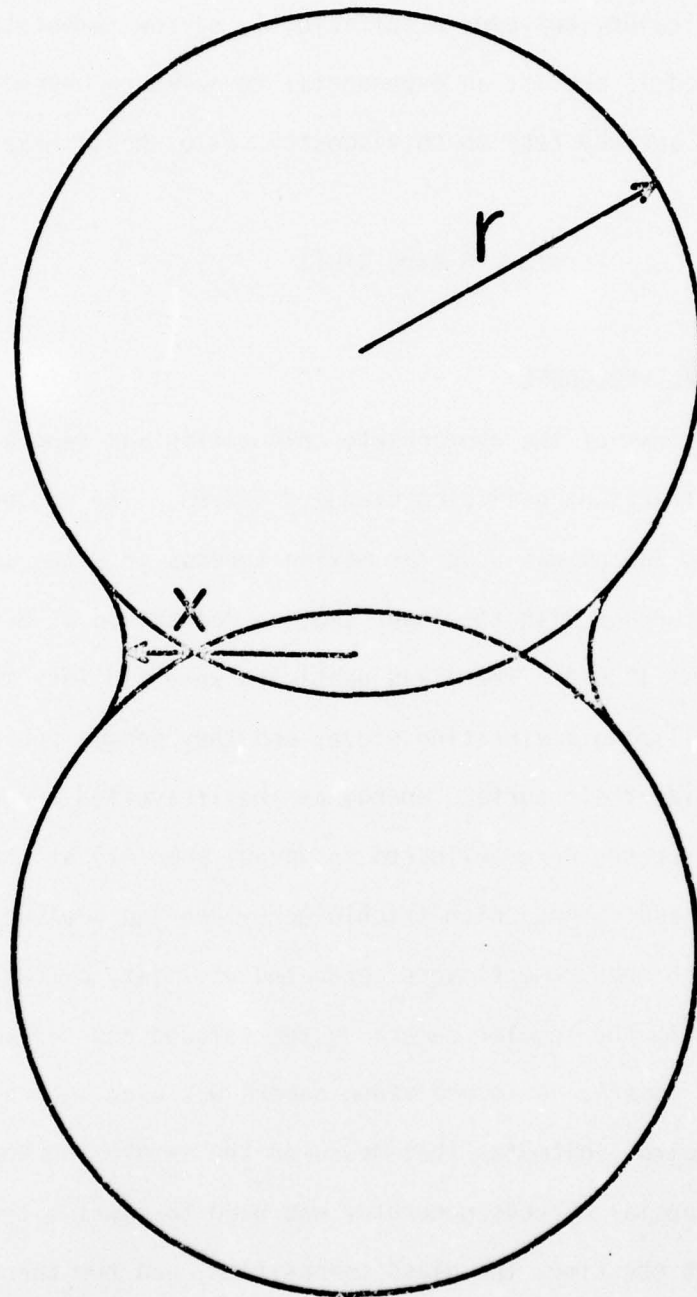


Figure III.1 Initial Stage of Viscous Flow Sintering

employed in the neck growth experiments, a constant surface tension is a good assumption, and all of the observed temperature dependence in  $\gamma/\eta$  can be attributed to the viscosity.

A number of theoretical models have been proposed to describe the viscosity of liquids, but over a sufficiently narrow temperature range, all of these models predict an exponential temperature dependence. Therefore, the surface tension to viscosity ratio should have the form:

$$\gamma/\eta = A \exp(-Q/RT) \quad (\text{III.3})$$

#### B. EXPERIMENTAL PROCEDURE

The glass frit of the appropriate composition was separated into particle size fractions utilizing standard sieves. The sieved fraction between 175 and 230  $\mu\text{m}$  was used for making spheres in a two section vertical tube furnace with the lower section maintained at 800°C and the upper section at 1200°C. The glass particles were fed into the top of the furnace utilizing a vibrating sieve, and they became spherical in order to minimize their surface energy as they travelled through the furnace. The spheres were collected in vacuum pump oil at the bottom of the furnace and cleaned with trichloroethylene and acetone.

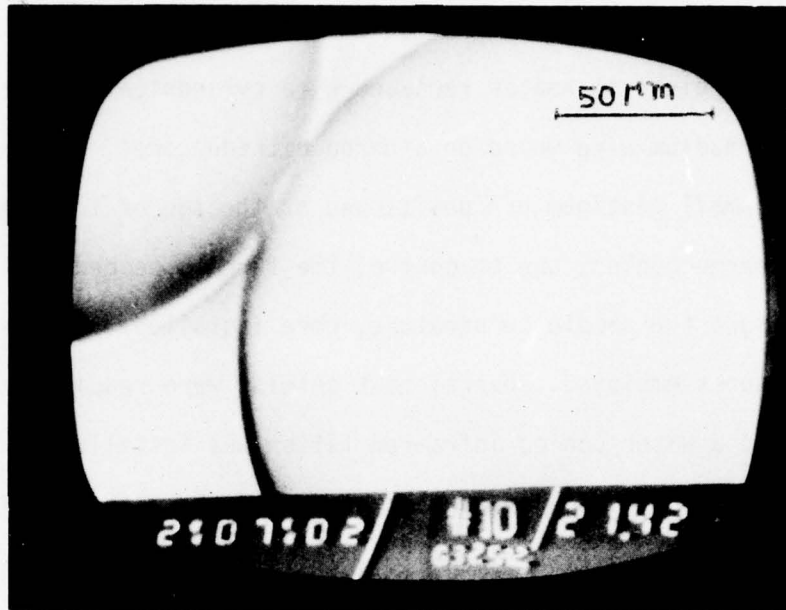
Neck growth measurements were conducted utilizing a modified hot stage metallograph with the regular camera system removed and replaced by a Sony AVC-3200 video camera. A second video camera was used to monitor a digital clock and a digital voltmeter that measured the sample thermocouple emf. A Sony SEG-1 special effects generator was used to combine the two video signals so that the time, the glass composition, and the thermocouple emf were positioned at the bottom of the image on the TV monitor screen. All information thus obtained was recorded on a Sony AV-3600 video recorder with stop frame capability, and observed on a Conrac SMA television monitor.

The hot stage unit was a modified Unitron HHS vacuum stage with the tungsten ribbon electric heater replaced by a cylindrical heater made of platinum-30% rhodium wire wound on a boron nitride core. The sample holder was a small platinum pan positioned at the top of the boron nitride core. Two thermocouples, one to control the furnace temperature and the other to measure the sample temperature, were installed. Because of the high temperatures employed, several heat shields were required inside the hot stage, and a water cooled infra-red filter was installed between the fused quartz viewing window of the hot stage and the objective lens. The objective lens used was a special focal length (Vickers M-02804) with a working distance of 14mm at 20X. A high intensity projector lamp with intensity control was used as the reflected light source.

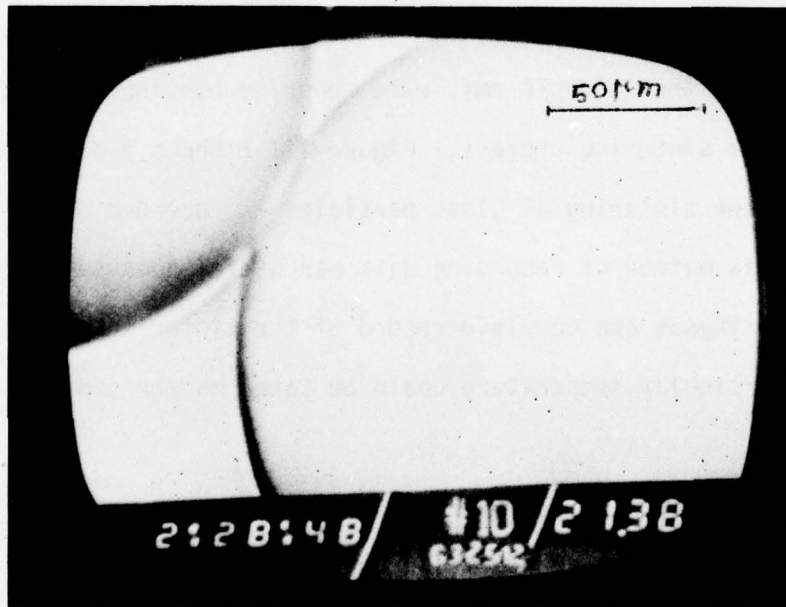
The experimental procedure consisted of placing a few glass spheres of similar size in the platinum pan of the hot stage unit and locating two particles touching each other for neck growth study. The furnace was heated to the required temperature and the neck growth data, including time and thermocouple emf, were recorded continuously on video tape during the sintering process. Figure III.2 shows two successive steps during the sintering of glass particles as recorded at one temperature. This method of recording data was useful because it created a virtually continuous and complete record of the sintering process and all data for a particular temperature could be taken on the same pair of glass spheres.

### C. RESULTS AND ANALYSIS

The results of neck growth measurements for five samples of each of the two 63-25-12 glasses and five samples of the 70-20-10 glasses are shown in Figs. III.3 - III.5. All data were well represented by a linear dependence of  $(x/r)^2$  on time at constant temperature. This is the



a. Relative time 0 min



b. Relative time 20 min, 46 seconds

Figure III.2 Initial Stage Sintering of 63-25-12 Glass Spheres at 503°C

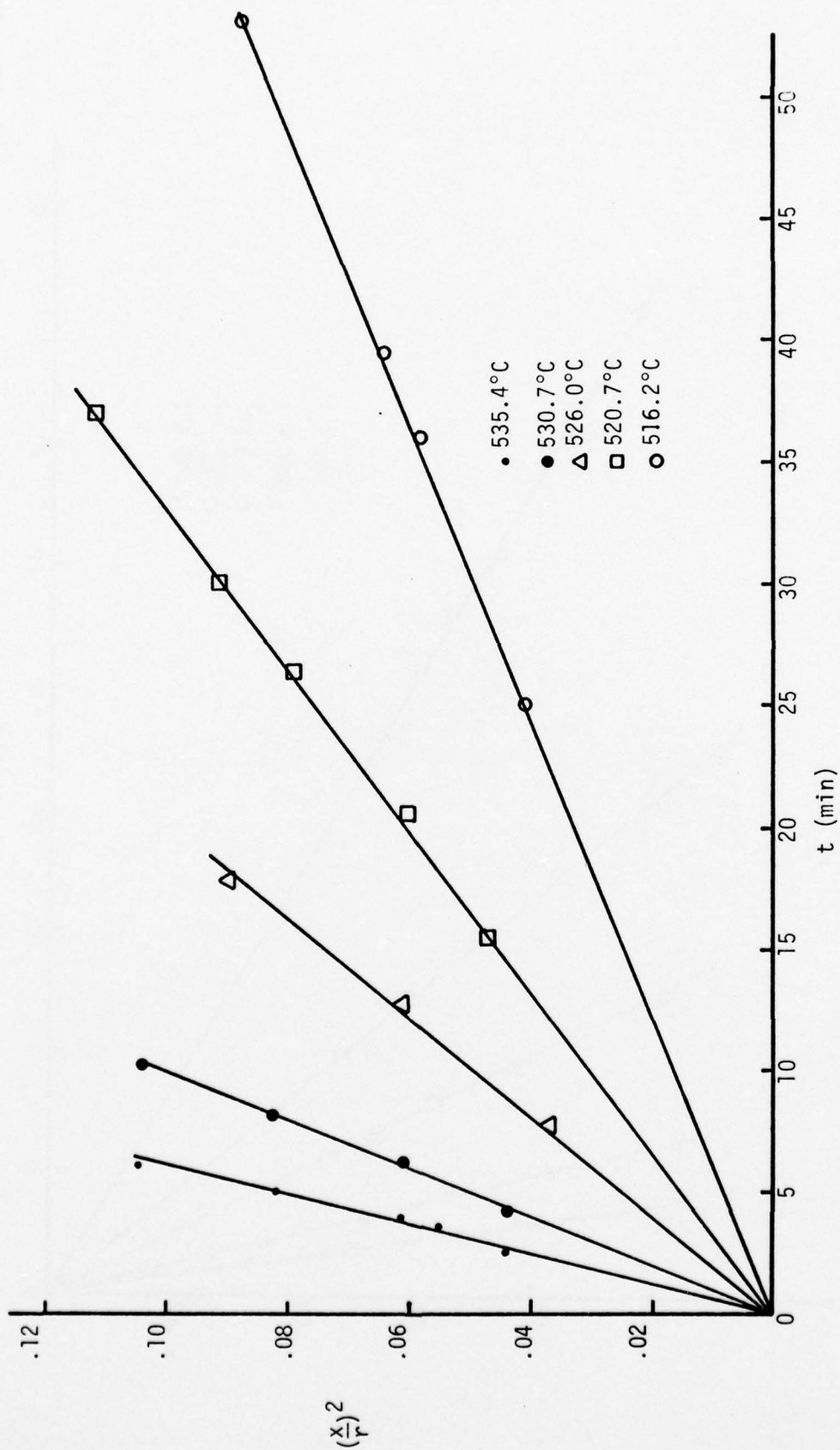


Figure III.3 Initial Stage Sintering Kinetics for Standard 63-25-12 Glass

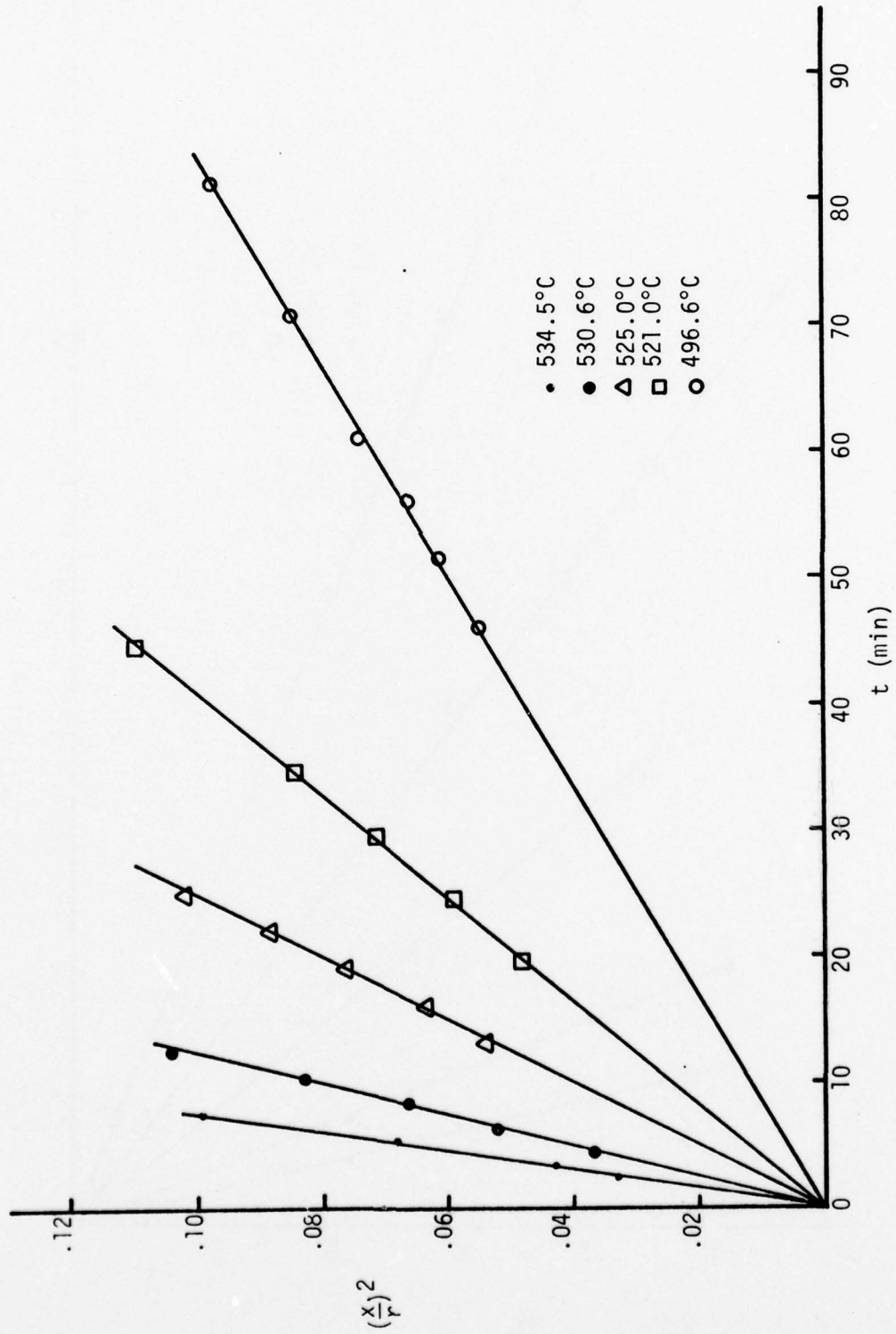


Figure III.4 Initial Stage Sintering Kinetics for 0-I 63-25-12 Glass

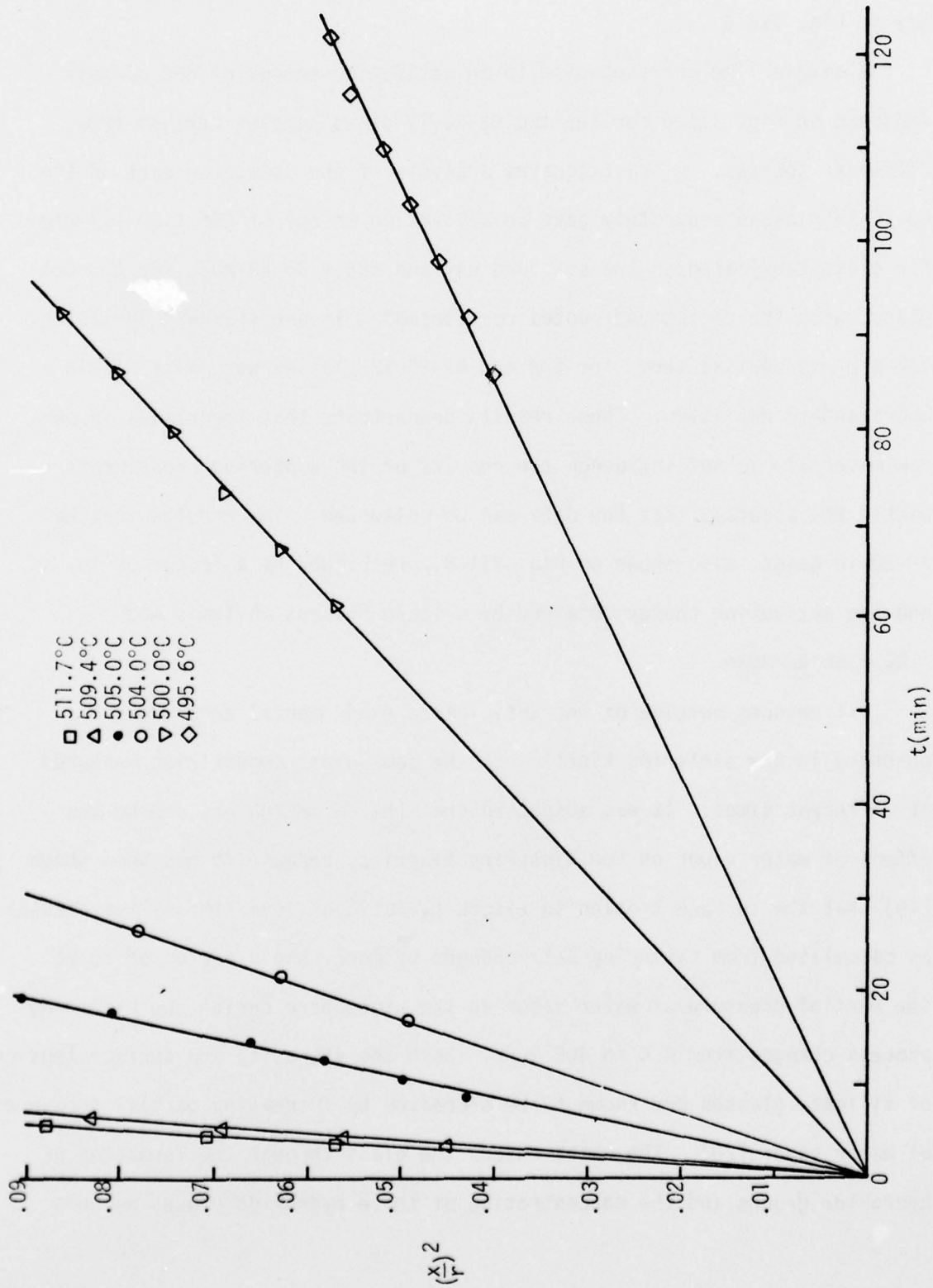


Figure III.5 Initial Stage Sintering Kinetics for Standard 70-20-10 Glass

behavior predicted by Eq. III.1, and the slope of each line on Figs. III.3 - III.5 will yield the surface tension to viscosity ratio. As discussed in Section IIIA, this ratio should have an exponential temperature dependence over a sufficiently small temperature range, and the data are plotted this way in Fig. III.6.

A single line corresponding to an activation energy of 666 kJ/mole is drawn on Fig. III.6 for the two 63-25-12 glass samples derived from different sources. A least squares analysis of the data from each of the 63-25-12 glasses separately gave an activation energy of  $646 \pm 39$  kJ/mole for glass fabricated in the standard way and  $686 \pm 35$  kJ/mole for the 0-I glass, with the variations quoted corresponding to one standard deviation. The pre-exponential terms for the two 62-25-12 glasses were also within one standard deviation. These results demonstrate that impurities in our raw materials do not influence the results of the sintering experiments within the accuracy that the data can be collected. The results for the 70-20-10 glass, also shown on Fig. III.6, are higher by a factor of 10 and the activation energy obtained by a least squares analysis was  $1180 \pm 66$  kJ/mole.

Differences outside of the anticipated experimental error were observed in the sintering kinetics of the same glass composition measured at different times. It was suspected that the variation was due to the effect of water vapor on the sintering kinetics, because it has been shown [19] that the surface tension to viscosity ratio of soda-lime-silica glasses as calculated from sintering data changes by more than a factor of 10 as the partial pressure of water vapor in the atmosphere during the sintering process changes from 4.6 to 405 torr. Both the viscosity and surface tension of silicate glasses are known to be decreased by increasing partial pressure of water vapor [20]. The water enters the glass through the formation of hydroxide groups and the concentration of these hydroxide groups depends

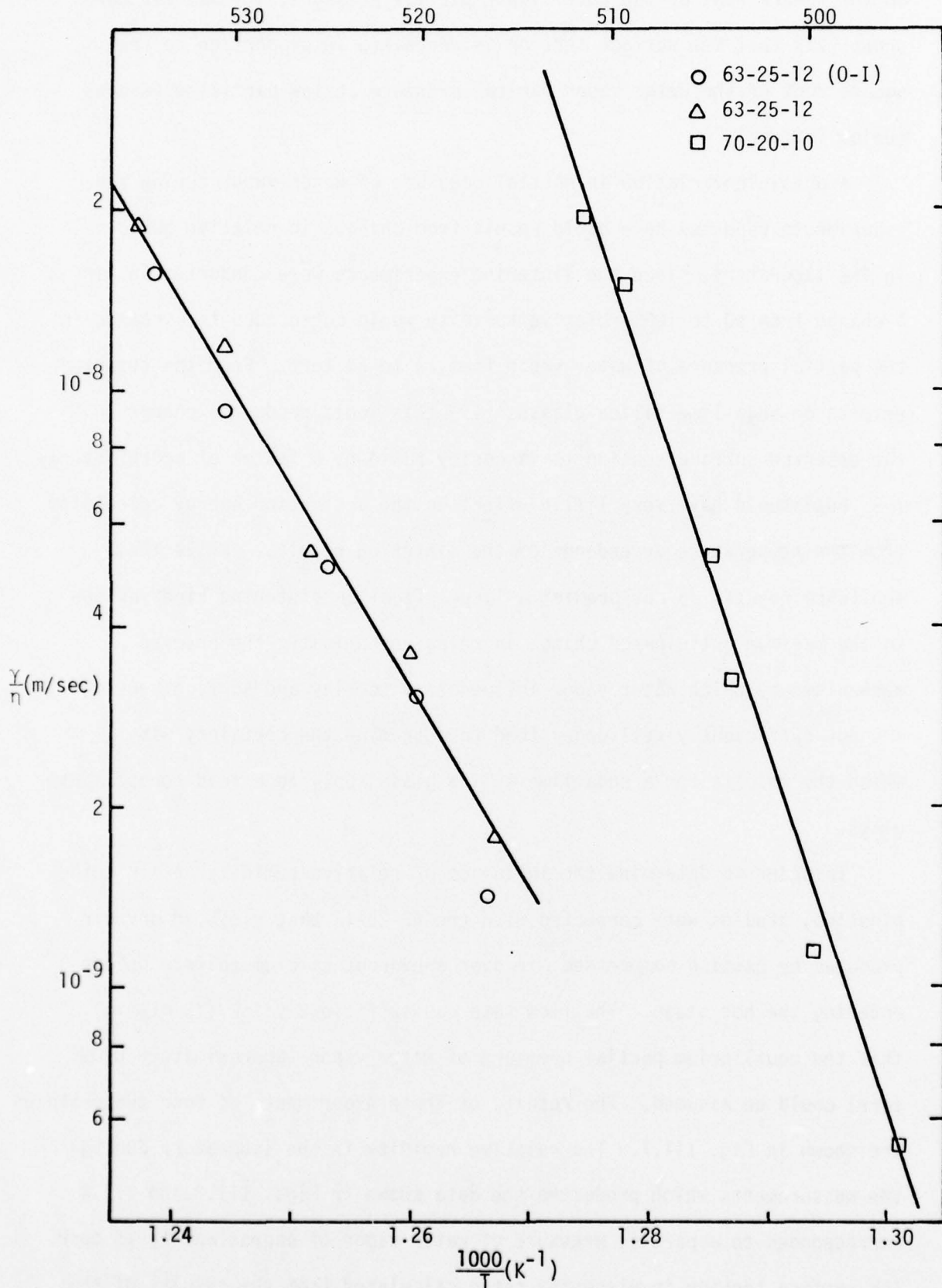


Figure III.6 Surface Tension to Viscosity Ratio for Base Glass Compositions

on the square root of the water vapor partial pressure. It has also been shown [21] that the surface tension is decreased in proportion to the square root of the water vapor partial pressure at low partial pressures (below 16 torr).

A possible variation in partial pressure of water vapor during the experiments reported here could result from changes in relative humidity in the laboratory, since the sintering experiments were conducted in air. A change from 50 to 100% relative humidity would correspond to a change in the partial pressure of water vapor from 12 to 24 torr. From the reported results on soda-lime-silica glasses [19] this would produce a change in the observed surface tension to viscosity ratio by a factor of approximately 1.3, but should have very little effect on the activation energy calculated from the temperature dependence of the sintering results. While these published results do not predict a large effect on sintering kinetics due to the maximum anticipated change in relative humidity, the precise mechanisms by which water vapor influences viscosity and surface tension are not sufficiently well understood to determine the certainty with which the results for a soda-lime-silica glass apply to a lead borosilicate glass.

In order to determine the influence of relative humidity on sintering kinetics, studies were conducted with the 63-25-12 base glass in dry air produced by passing compressed air over anhydrous calcium sulfate before entering the hot stage. The flow rate was sufficiently low (15 ml/min) that the equilibrium partial pressure of water vapor (approximately 0.005 torr) could be assumed. The results of these experiments at four temperatures are shown in Fig. III.7. The relative humidity in the laboratory during the measurements which produced the data shown in Figs. III.3 and III.4 corresponded to a partial pressure of water vapor of approximately 15 torr. The surface tension to viscosity ratio calculated from the results of the

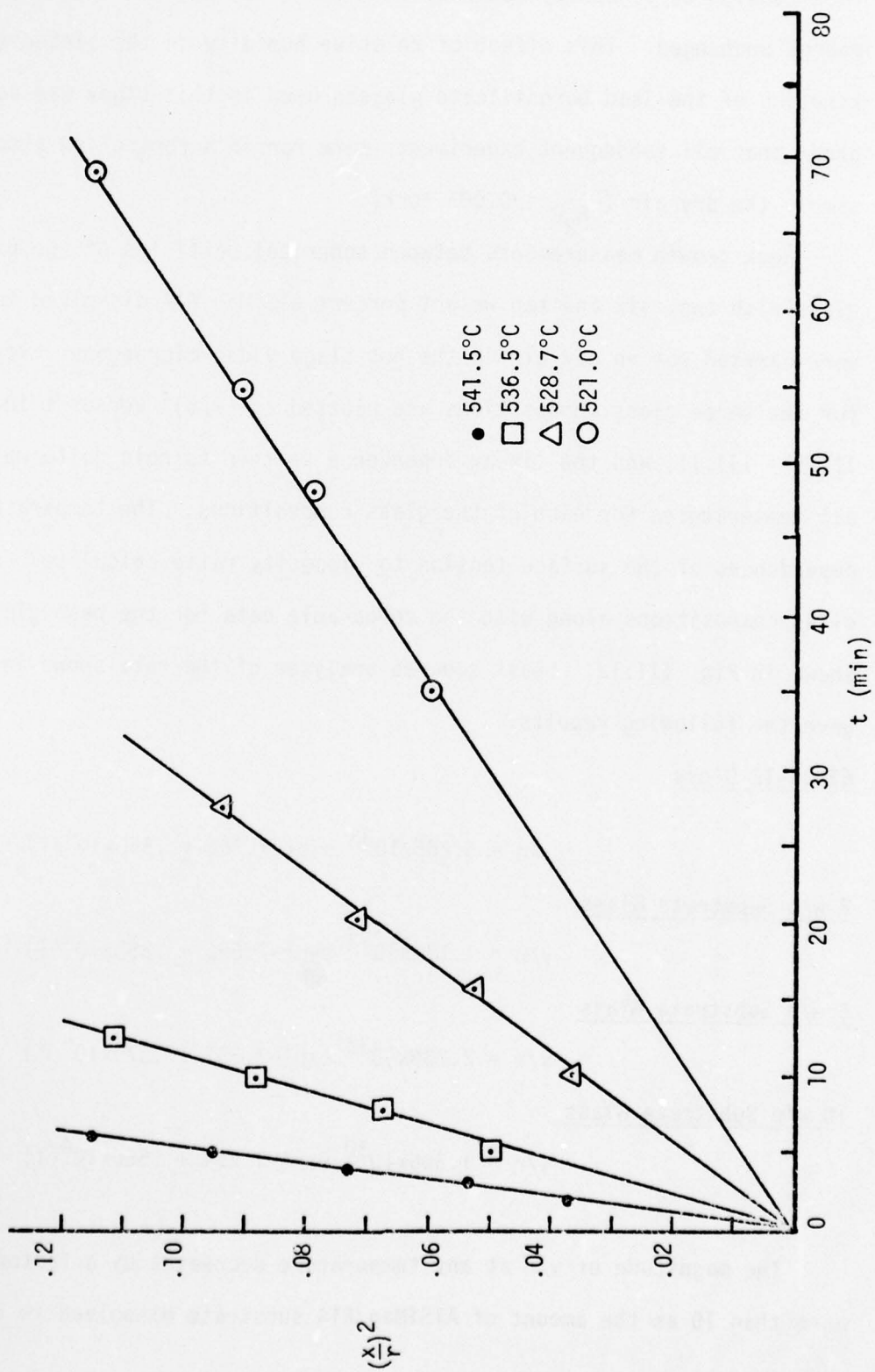


Figure III.7 Initial Stage Sintering Kinetics for 63-25-12 Glass in Dry Air

experiments in the two atmospheres are shown in Fig. III.8. The effect of this variation in moisture content of the atmosphere is to change the surface tension to viscosity ratio by a factor of 2, but to leave the activation energy unchanged. This effect of relative humidity on the sintering kinetics of the lead borosilicate glasses used in this study was sufficiently great that all subsequent experiments were run in a controlled atmosphere, namely the dry air ( $P_{H_2O} = 0.005$  torr).

Neck growth measurements between spherical particles of the 63-25-12 glass with two, six and ten weight percent AlSiMag 614 dissolved in it were carried out in dry air in the hot stage video microscope. Results for the three glass compositions are plotted as  $(x/r)^2$  versus  $t$  in Figs. III.9 - III.11, and the linear dependence is seen to hold quite well at all temperatures for each of the glass compositions. The temperature dependences of the surface tension to viscosity ratio calculated for these glass compositions along with the comparable data for the base glass are shown in Fig. III.12. Least squares analyses of the data shown in Fig. III.12 gave the following results.

63-25-12 Glass

$$\gamma/\eta = 5.265 \times 10^{33} \exp(-7.764 \pm .558 \times 10^4/T) \quad (\text{III.4})$$

2 w/o Substrate Glass

$$\gamma/\eta = 1.178 \times 10^{33} \exp(-7.656 \pm .258 \times 10^4/T) \quad (\text{III.5})$$

6 w/o Substrate Glass

$$\gamma/\eta = 2.239 \times 10^{32} \exp(-7.587 \pm .579 \times 10^4/T) \quad (\text{III.6})$$

10 w/o Substrate Glass

$$\gamma/\eta = 1.306 \times 10^{30} \exp(-7.264 \pm .550 \times 10^4/T) \quad (\text{III.7})$$

The magnitude of  $\gamma/\eta$  at any temperature decreases by a factor of more than 10 as the amount of AlSiMag 614 substrate dissolved in 63-25-12

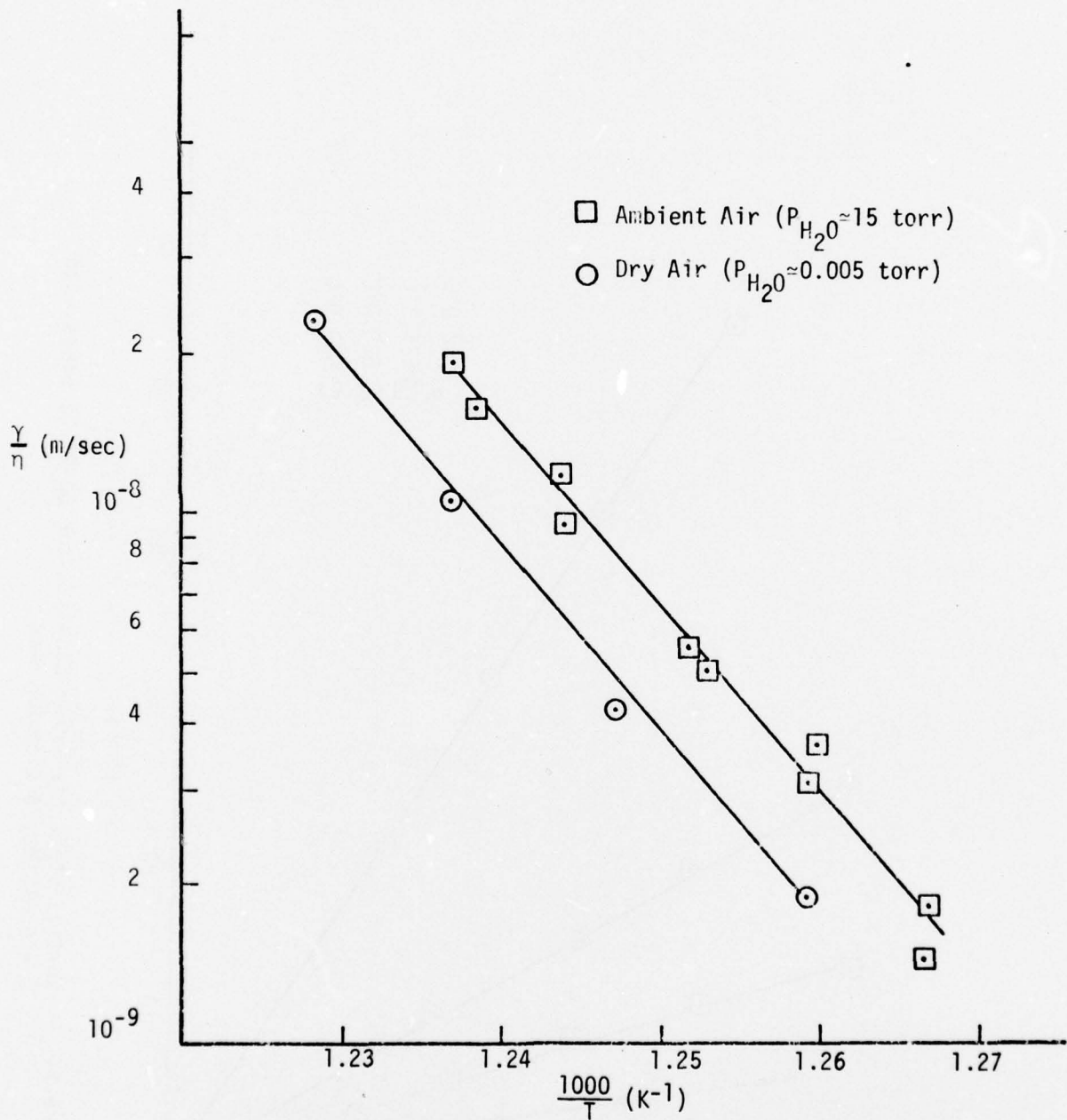


Figure III.8 Effect of Relative Humidity on Surface Tension to Viscosity Ratio of 63-25-12 Glass

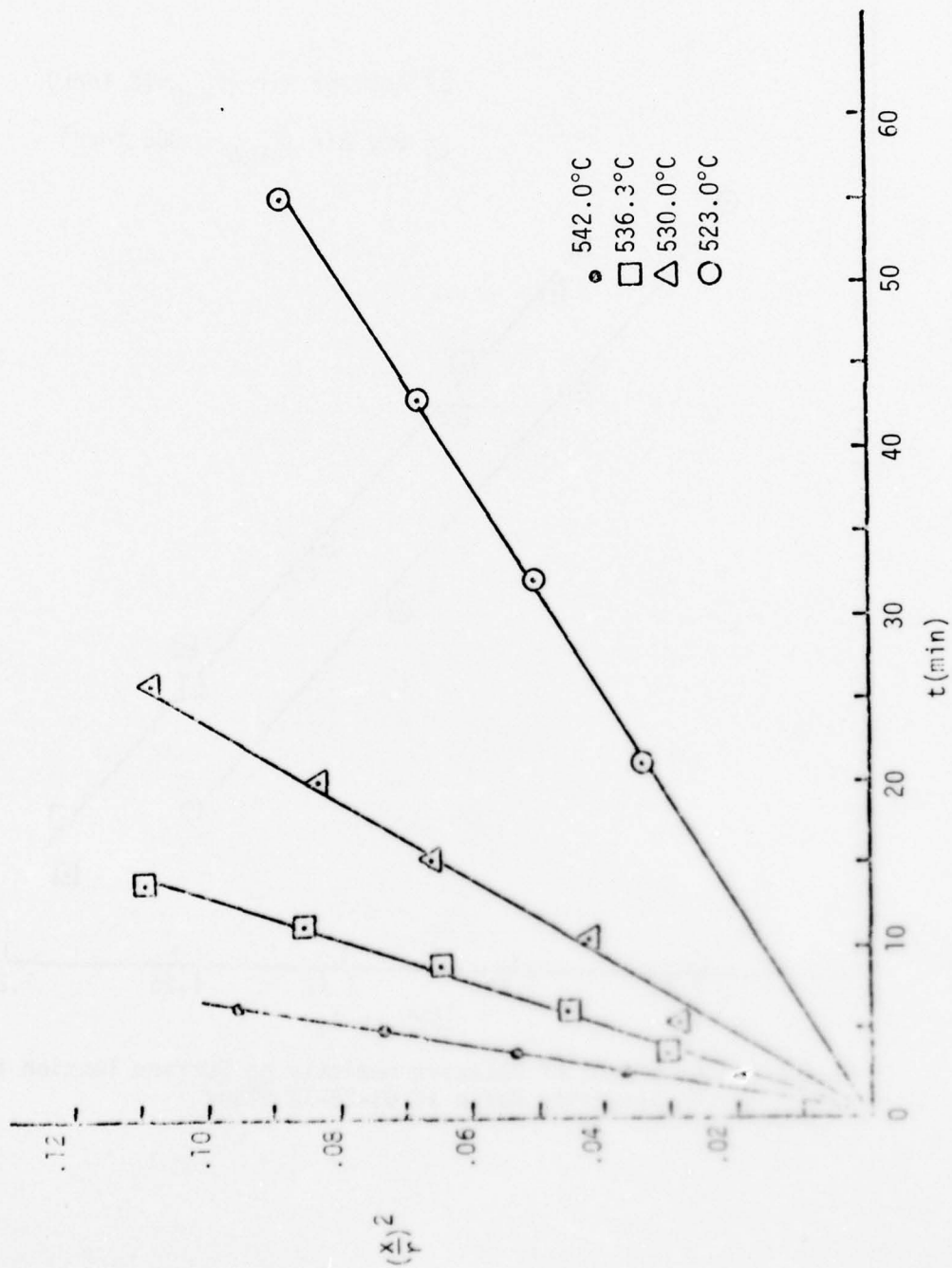


Figure III.9 Initial Stage Sintering Kinetics for 63-25-12 Glass with 2 w/o AlSiMag 614 in Dry Air

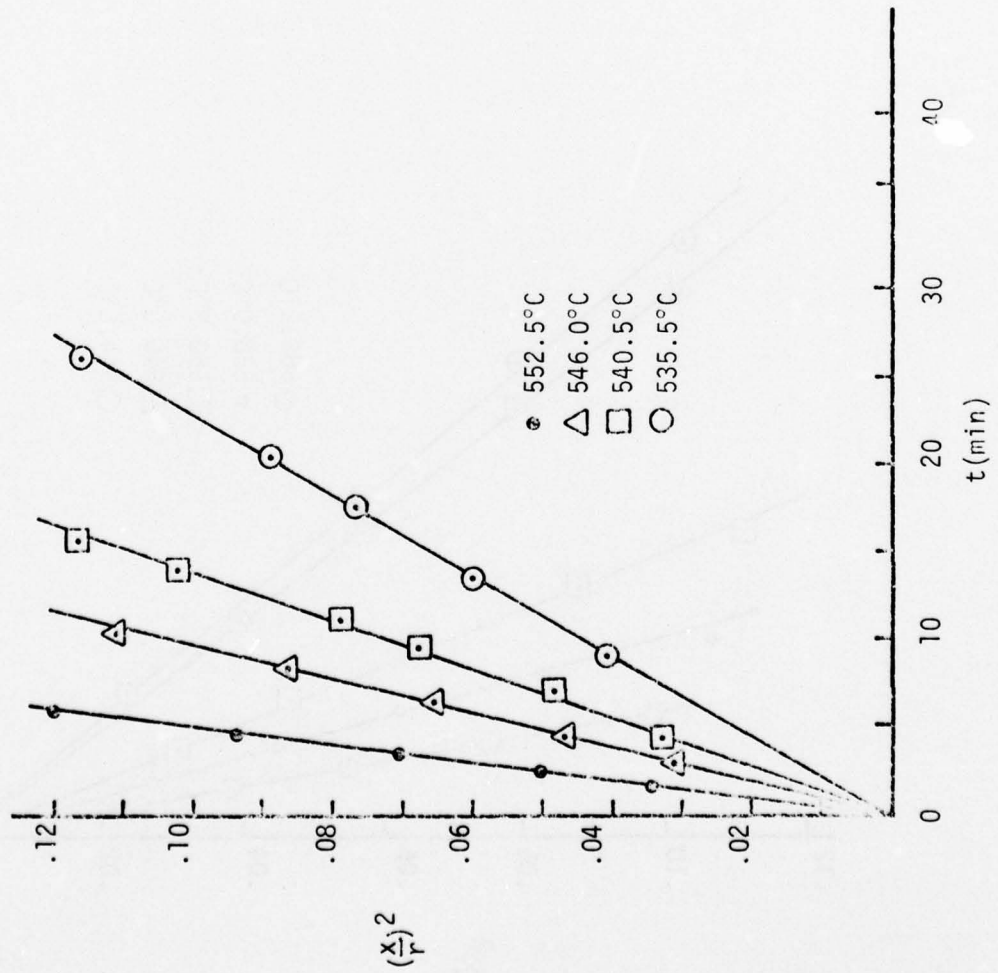


Figure III.10 Initial Stage Sintering Kinetics for 63-25-12 Glass with 6 w/o AlSiMag 614 in Dry Air

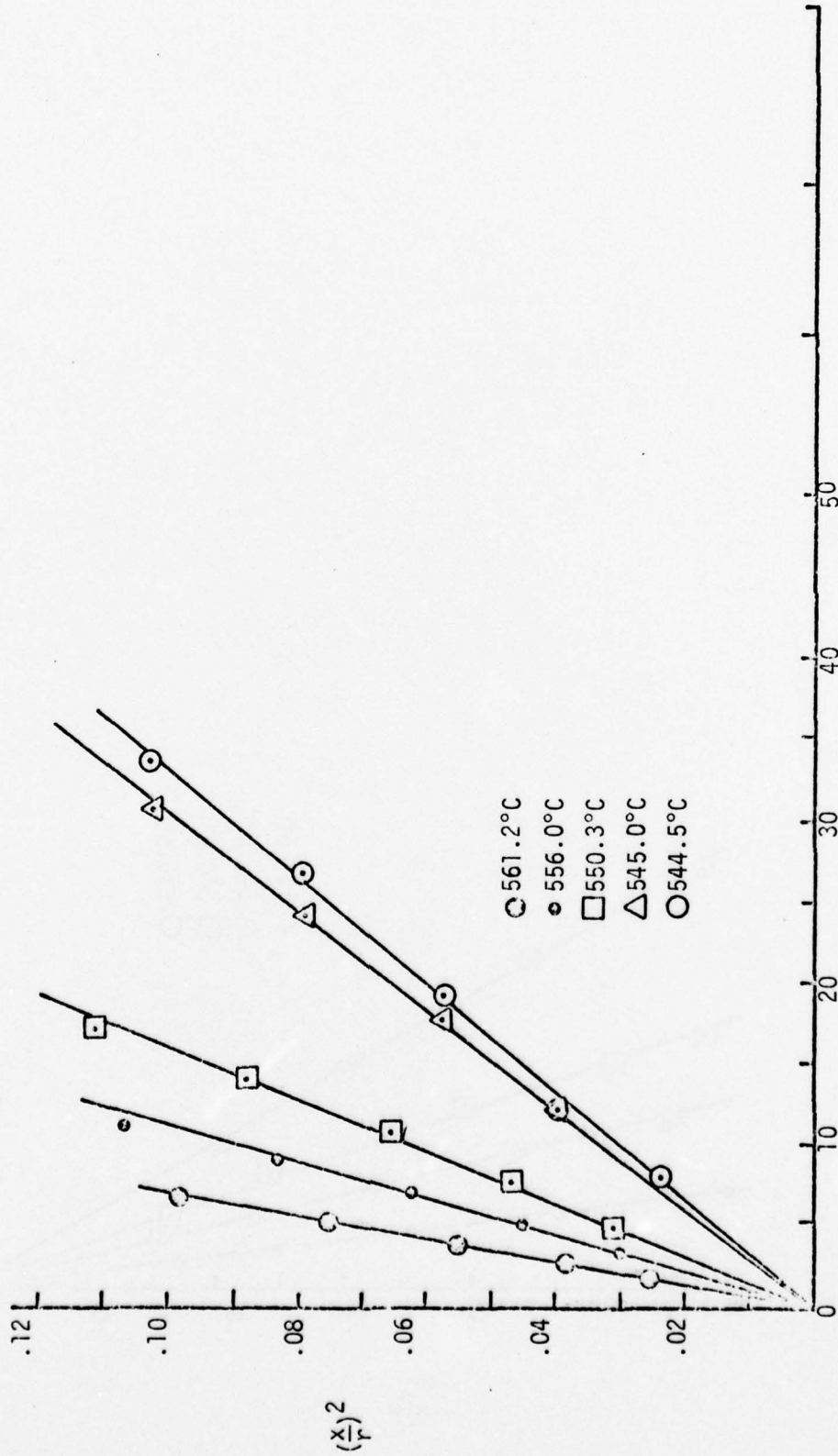


Figure III.11 Initial Stage Sintering Kinetics for 63-25-12 Glass with 10 w/o AlSiMag 614 in Dry Air

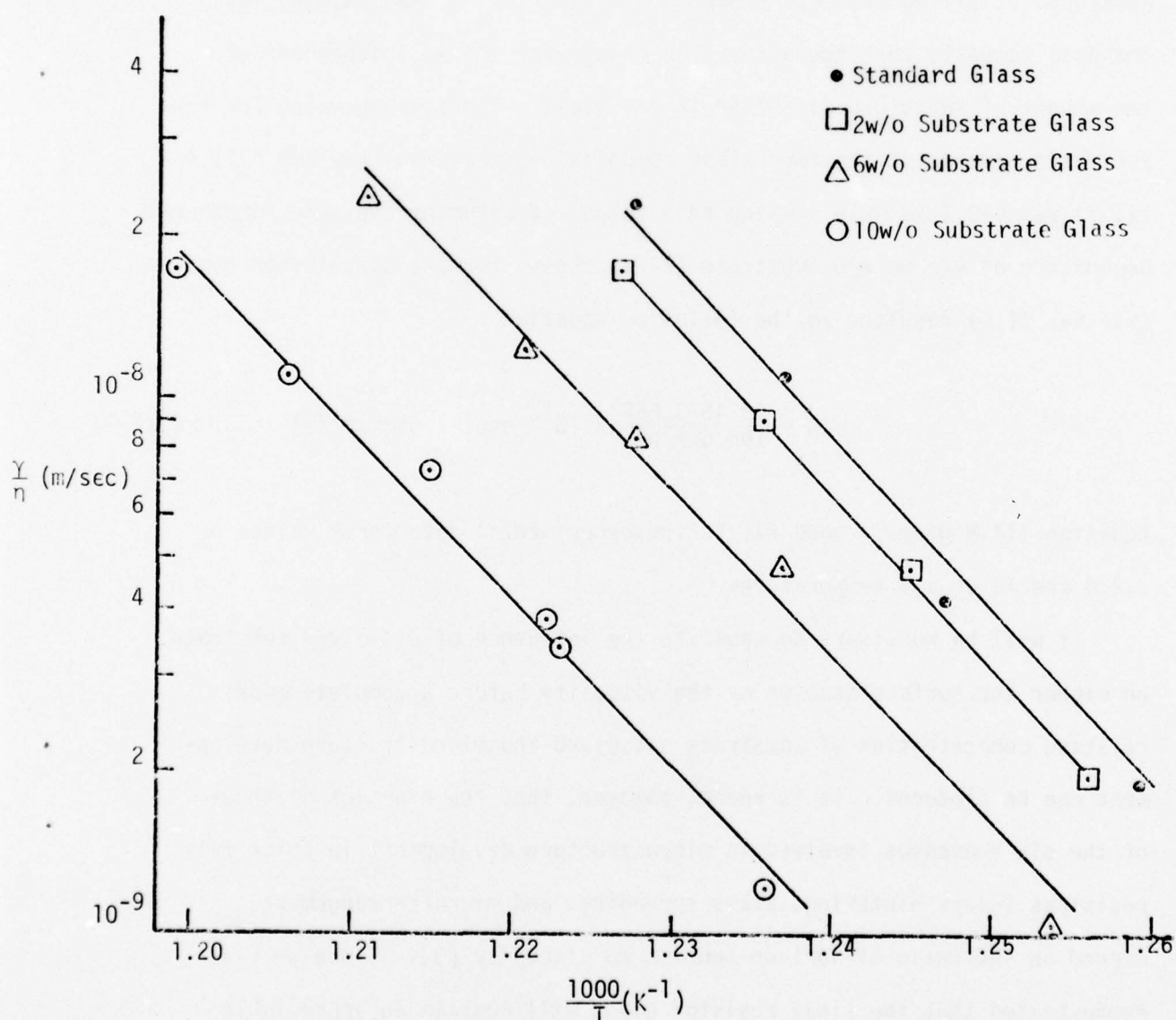


Figure III.12 Effect of Dissolved AlSiMag 614 on Surface Tension to Viscosity Ratio of 63-25-12 Glass

glass is increased from zero to 10 w/o, but the activation energies indicated in Eqs. III.4 - III.7 are all within one standard deviation of each other.

#### D. DISCUSSION

An empirical equation describing the dependence of surface tension to viscosity ratio on amount of substrate dissolved in the glass can be developed utilizing the data shown in Fig. III.12. It was assumed, as the data suggest, that the activation energy for  $\gamma/\eta$  is independent of the amount of substrate dissolved in the glass. The average value for the activation energy of the four glass compositions measured (see Eqs. III.4 - III.7) was 630.7 kJ/mole. Using this value and assuming the same functional dependence of  $\gamma/\eta$  on w/o substrate (P) as chosen for the dissolution rate (see Eq. II.5) resulted in the following equation.

$$\gamma/\eta = \frac{49.45-3.86P}{108.6 + P^2} \times 10^{33} \exp(-7.568 \times 10^4/T) \quad (\text{III.8})$$

Equation III.8 gives a good fit to the experimental data for P values of 0,2,6 and 10 at all temperatures.

It will be necessary to separate the influence of dissolved substrate on either the surface tension or the viscosity before a complete model relating concentration of substrate dissolved and microstructure development can be produced. It is known, however, that the kinetics of three of the six processes involved in microstructure development in thick film resistors (glass sintering, glass spreading, and microrearrangement) depend on the ratio of surface tension to viscosity [3]. Since we have demonstrated that the final resistor glass will contain an appreciable amount of dissolved substrate after processing at standard conditions, it is apparent that the important microstructure development processes will reach varying stages of completion depending upon the amount of substrate

dissolved in the glass during processing. This effect can be taken into account by solving Eq. II.8 to obtain the amount of substrate recession at any time and temperature, substituting this value of  $Y$  in Eq. II.7 to obtain the corresponding weight percent substrate dissolved in the glass, and using this value of  $P$  in Eq. III.8 to determine the surface tension to viscosity ratio.

#### IV. ELECTRICAL EFFECTS

##### A. EXPERIMENTAL PROCEDURE

###### 1. Resistors

Previous studies [4] of changes in electrical properties due to varying amounts of AlSiMag 614 substrate dissolved in 70-20-10 glass were conducted with cylindrical samples prepared by firing compressed pellets of RuO<sub>2</sub>-glass mixtures in platinum boats. The composites were removed from the foil, annealed, and leads attached. While this method produced workable resistors that clearly showed different characteristics for 70-20-10 glasses having varying amounts of substrate dissolved, the geometry was considerably different than a thick film resistor and the influence of resistor thickness on the kinetics of microstructure development is not sufficiently well known to allow for extrapolations. It was therefore desired to verify these results using a fabrication procedure which more closely simulated the techniques used in the thick film industry, but without introducing resistor-substrate interactions, and to repeat the studies with the 63-25-12 base glass.

The mixed powders containing 5 or 10 w/o RuO<sub>2</sub> relative to glass were blended with 60 volume percent screening agent (10 w/o N-300 ethyl cellulose dissolved in butyl carbitol solvent). The formulation was thoroughly blended on a silica glass sleeved roll mill and stored in air tight glass jars. The substrates for screening and firing resistors were made by wrapping thin (76 μm) platinum foil around alumina substrates (1.3x13x13 mm). The foil allowed the resistor to be fired without reacting with the substrate, while the alumina substrate provided mechanical strength to the assembly during processing. The formulation was screened onto the platinum foil in a rectangular pattern 4 x 12 mm. After screening, the ink was dried at

240°C for 15 minutes to remove the butyl carbitol, and the procedure repeated until the resistor had 4 screened layers. The multi layers were necessary for mechanical strength. The resistors were fired, one at a time, in a push-rod furnace using an initial heating rate of 50° per minute to 500°C, a 10 minute hold at 500°C, a heat at 60° per minute to 800°C, a 10 minute hold, and a cool to room temperature at 160° per minute. The 500°C constant temperature region was necessary in order to completely remove the ethyl cellulose. The difference in coefficient of thermal expansion between the glass in the resistor and platinum was such that appreciable thermal stresses were developed, but these were not sufficient to cause fracture in the resistor films. The platinum foil was removed from the fired resistor by first gluing the top of the resistor to a microscope slide with wax. The platinum foil was straightened, the alumina substrate lifted out, and the platinum foil gently peeled off to leave the resistor embedded in the wax. To remove the wax, the glass slide was placed in trichlorethylene until the resistor released from the slide. The resistor was then rinsed at least 10 times in trichloroethylene to remove all traces of wax. The cleaned resistors were approximately 125  $\mu\text{m}$  thick.

In order to provide mechanical strength and to remove residual stresses, it was desirable to sinter the resistors onto appropriate substrates and simultaneously anneal them. Three different substrates were evaluated for this application: AlSiMag 614; AlSiMag 614 preglazed with the same glass composition; and platinum foil preglazed with the same glass composition. Since sintering occurs in the neighborhood of the softening point of glass which is considerably below normal processing temperatures, there would be negligible composition variation during bonding with any substrate. For the resistors made with either of the base glasses, an annealing temperature of 450°C for 1 hour provided good bonding between the resistor and the substrate. A somewhat higher temperature was needed for resistors using

glass with dissolved substrate because of the increased softening point of the glass composition. Electrical leads were then attached to the resistor by one of two methods; platinum wires were attached using silver epoxy, or platinum electrodes were deposited by RF sputtering.

Considerable difficulties were encountered in producing stable, reproducible resistors made with 70-20-10 glass and sintered on AlSiMag 614 substrates. These difficulties were traced to the development of cracks in the resistor at some point during the fabrication procedure. Controlled experiments were performed to isolate the source of the cracking, and the problem was found to occur during the sintering step. Glazing AlSiMag 614 substrates with the 70-20-10 glass before sintering the resistor in place was attempted in order to circumvent the problem, but the glaze as well as resistor was found to develop small cracks on cooling. Successful resistors were fabricated by sintering them to platinum foil which had previously been glazed with 70-20-10 glass to provide electrical insulation.

Three different types of substrates were evaluated for resistors made with 63-25-12 glass: (1) AlSiMag 614 substrates with fired platinum electrodes; (2) AlSiMag 614 substrates preglazed with 63-25-12 glass; and (3) AlSiMag 614 substrates alone. Devices sintered to substrates with fired platinum electrodes were found to be unstable due to poor electrical contact at the resistor-conductive interface. Difficulties were also encountered with the stability of the devices sintered to pre-glazed substrates. It was found that sintering the resistors on plain AlSiMag 614 substrates gave stable resistors which exhibited no cracking. In addition, resistors were made with 63-25-12 glass without a sinter or anneal step. After removing the fired resistors from the platinum foil, platinum leads were attached using a conducting epoxy, and electrical measurements were made with the resistors lying on, but not sintered to, AlSiMag 614 substrates.

## 2. MIM DEVICE FABRICATION

Branches of the conducting chains of  $\text{RuO}_2$  in thick film resistors are sometimes separated by a thin layer of glass. In order to determine the effects of the composition of this glass on the electrical properties of the resistors, it is first necessary to characterize the electrical properties (bulk resistivity, dielectric constant, and dielectric strength) of the glass itself as a function of composition (amount of dissolved substrate). Most of these properties, in addition to the tunneling and emission characteristics, can be measured using a standard metal-oxide-metal (MIM) structure. The desired MIM structures are platinum-glass-platinum, platinum-glass- $\text{RuO}_2$  and  $\text{RuO}_2$ -glass- $\text{RuO}_2$ . The primary experimental efforts have been devoted to the development of techniques for sputtering glass films in the thickness range 10-1000 Å.

The initial efforts at fabricating the MIM device were centered on the development of techniques for sputtering the glass without changing its chemical composition. Preliminary results using an argon atmosphere indicated an apparent reduction of the glass, presumably due to the formation of elemental lead. This was observed as a color change in the glass target from white to black. Subsequent experiments using a 20% oxygen, 80% argon atmosphere showed improvement, but still some darkening of the glass target. An atmosphere of 50% oxygen, 50% argon together with the optimization of all sputtering parameters including input power, source to substrate spacing and substrate temperature yielded glass films with no apparent reduction. A post-sputtering anneal may still be required in order to define the oxygen stoichiometry of the glass.

Progress in producing sputtered glass devices took a major step forward with the development of a technique for casting the glass targets. Spraying 325 mesh glass powders gave a very porous target surface but not enough adhesion to the aluminium back plate. Screening the glass powders

and doctor-blading powders gave more dense films but they tended to crack during drying to volatilize organics. The cast glass targets were smooth, clear, bubble-free disks 12.5 cm in diameter and approximately 3 mm thick. These were fabricated by pre-heating a stainless steel mold to about 400°C, melting the appropriate glass composition at 900°C in a platinum crucible and pouring the glass into the mold. The mold was then covered and kept at 400°C for 1 hour, before air-cooling to room temperature. Because the edge of mold was slightly beveled the glass targets could be easily removed without using any mold release compounds. The targets were then annealed at 425°C for 24 hours to relieve any stresses. After cleaning, the targets were mounted onto aluminum blanks with epoxy.

Glass films have been sputtered on three separate occasions and certain of the system sputtering parameters necessary for obtaining optimum films have been determined. At a forward power of 400 watts in an atmosphere containing equal amounts of oxygen and argon at a total pressure of  $7.0 \times 10^{-3}$  torr, a sputtering rate of  $30 \text{ \AA}/\text{min}$  has been established. This slow rate will be beneficial in obtaining very thin oxides necessary to measure tunneling currents.

The MIM devices involving platinum are fabricated by first sputtering a layer of platinum onto an oxidized silicon wafer. The glass is sputtered onto the platinum then counter-electrodes of platinum are sputtered on top for the platinum-glass-platinum devices. It was found that platinum sputtered in an argon atmosphere at  $1.4 \times 10^{-2}$  torr with a forward power of 400 watts produced a sputtering rate of  $1300 \text{ \AA}/\text{min}$ . After analysis of the first 3 glass sputtering runs, it was determined that the sputtering rate of the platinum should be reduced because the platinum splattered the  $\text{SiO}_2$  film causing a very uneven surface, poor adhesion of the platinum film, and areas of possible failure of the MIM device.

The next step in device fabrication will be to determine the comp-

osition of the sputtered film, specifically the oxygen content. This will be done using a SIMS system. Composition of starting glass, sputtered film, and sputtered films of various annealed states will be analyzed to optimize sputtering and annealing steps of fabrication.

## B. RESULTS AND ANALYSIS

### 1. 70-20-10 Base Glass

Resistor formulations were prepared using 5 w/o  $\text{RuO}_2$  relative to 70-20-10 glass, and 5 w/o  $\text{RuO}_2$  relative to 70-20-10 glass containing 8 w/o dissolved AlSiMag 614 substrate. These formulations were printed and fired on platinum foil, and then the resistors sintered onto glazed platinum substrates. Resistors made with glass containing dissolved substrate exhibited a room temperature resistivity higher by a factor of 2 than resistors made using glass with no dissolved substrate. The temperature dependence of the resistance was also considerably different as is shown in Fig. IV.1 where the normalized resistance is plotted as a function of temperature. The resistors made from glass containing no dissolved substrate had a TCR of approximately 400 ppm/°C up to 90°C as compared to less than 100 ppm/°C for the resistors fabricated from glass having 8 w/o dissolved substrate. In both cases, the normalized resistance increased more rapidly at higher temperatures which is typical of thick film resistor behavior. These results are very similar to those obtained with composites made from  $\text{RuO}_2$  and 70-20-10 glass with and without dissolved substrate [4].

### 2. 63-25-12 Base Glass

Resistor formulations were prepared using 5 w/o  $\text{RuO}_2$  relative to 63-25-12 glass, and 5 w/o  $\text{RuO}_2$  relative to 63-25-12 glass containing 10 w/o dissolved AlSiMag 614 substrate. These formulations were printed and fired on platinum foil and then the resistors sintered onto AlSiMag 614 substrates.

Current-voltage measurements were conducted on several devices,

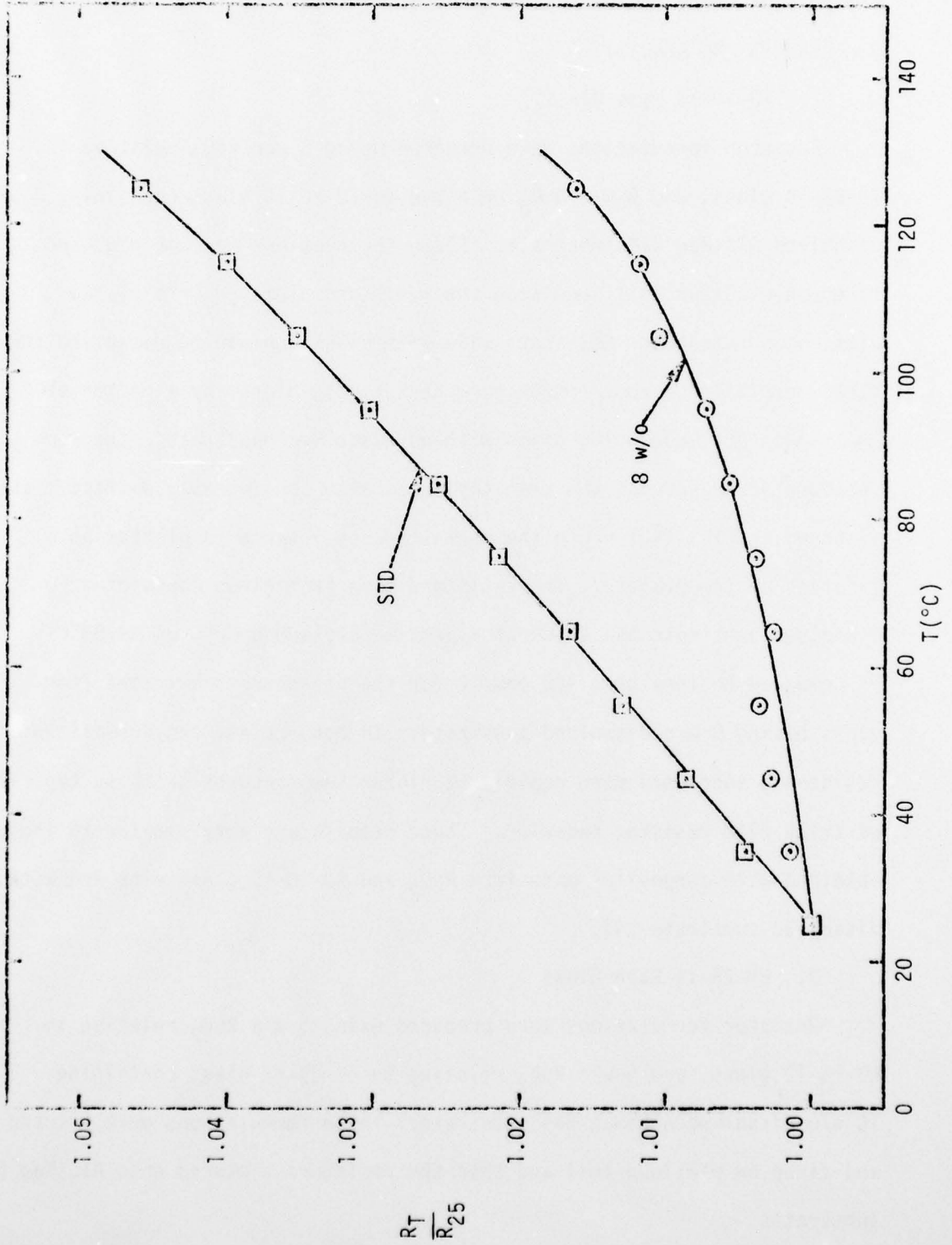


Figure IV.1 Effect of 8 w/o AlSiMag 614 in 70-20-10 Glass on 5 w/o RuO2 Resistors Sintered on Glazed Platinum Substrates - TCR

and a linear behavior over 6 orders of magnitude using either forward or reverse polarity was observed in all cases. The data for two resistors made with standard glass and two with the 10 w/o substrate glass are shown in Fig. IV.2. The resistors fabricated from glass containing 10 w/o dissolved substrate showed a room temperature resistance that was higher by a factor of approximately 100 compared to the resistors fabricated with pure 63-25-12 glass. The temperature dependence of the sheet resistance relative to its value at room temperature for two standard glass resistors and two 10 w/o substrate glass resistors is shown in Fig. IV.3. All resistors fabricated from 10 w/o substrate glass were very stable and gave highly reproducible data over the temperature range  $-55^{\circ}$  to  $125^{\circ}\text{C}$ . However, the resistors fabricated with 63-25-12 glass containing no dissolved substrate exhibited a much more erratic behavior during temperature cycling with the resistance increasing very sharply below room temperature. Curves are drawn at the low temperatures for the standard glass resistors to indicate the general behavior, but considerable variations were observed on thermal cycling and reproducible data could not be obtained. Representative values for hot and cold TCR for the four resistors shown in Fig. IV.3 are given in the following table:

<u>Resistor No.</u>	<u>HOT(<math>25^{\circ}</math> - <math>125^{\circ}\text{C}</math>)TCR</u>	<u>COLD(<math>-55^{\circ}</math> - <math>25^{\circ}\text{C}</math>)TCR</u>
STD-02	+120 ppm/ $^{\circ}\text{C}$	-11,500 ppm/ $^{\circ}\text{C}$
STD-04	+240 ppm/ $^{\circ}\text{C}$	-5,500 ppm/ $^{\circ}\text{C}$
10 w/o-01	+30 ppm/ $^{\circ}\text{C}$	-100 ppm/ $^{\circ}\text{C}$
10 w/o-04	+15 ppm/ $^{\circ}\text{C}$	-50 ppm/ $^{\circ}\text{C}$

Resistors were fabricated from the 63-25-12 inks in the same manor as described above except that the sintering step was not included. Representative data for the relative resistance as a function of temperature for the

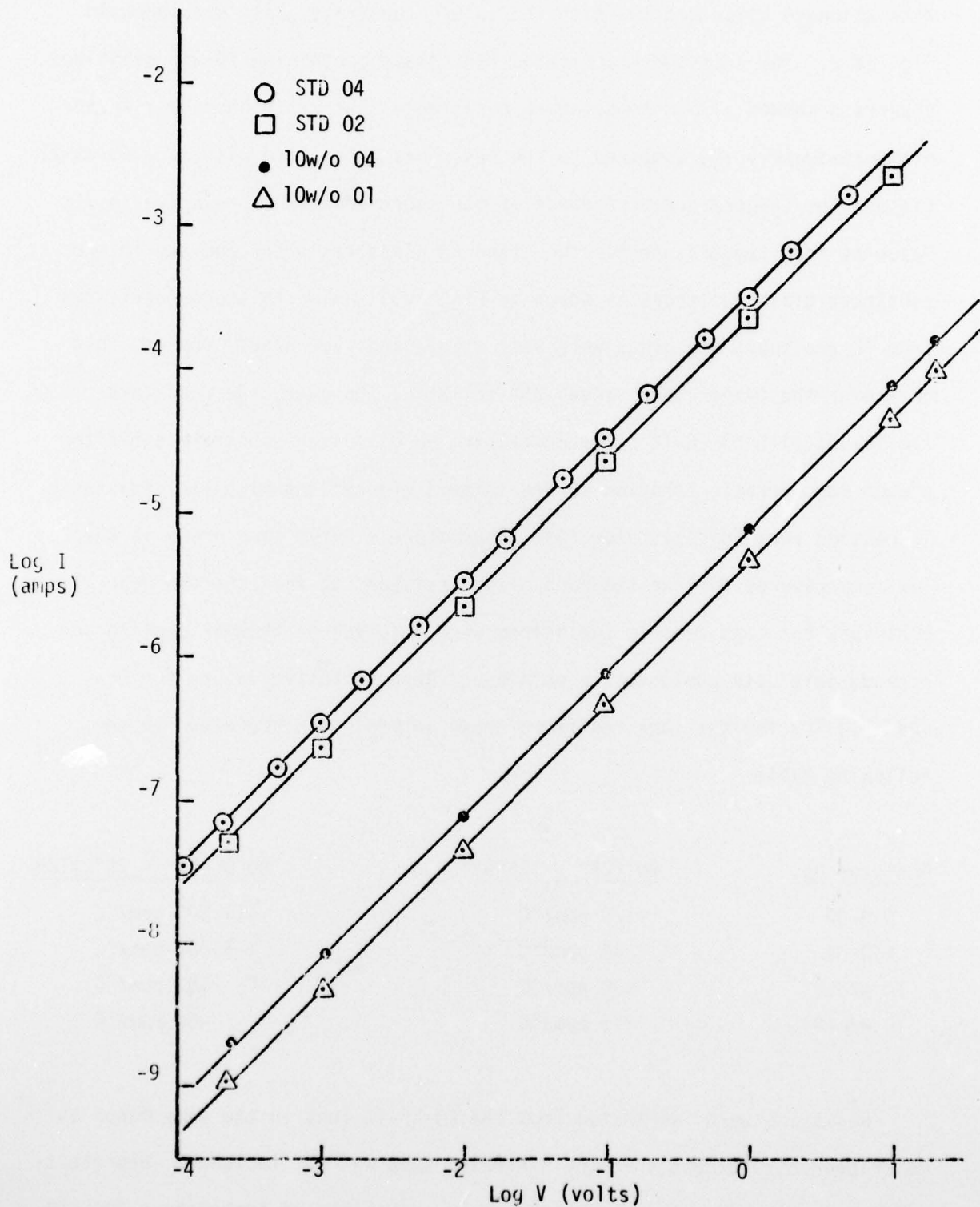


Figure IV.2 Effect of 10w/o AlSiMag 614 in 63-25-12 Glass on 5w/o RuO<sub>2</sub> Resistors Sintered on AlSiMag 614 Substrates - Sheet Resistance and VCR

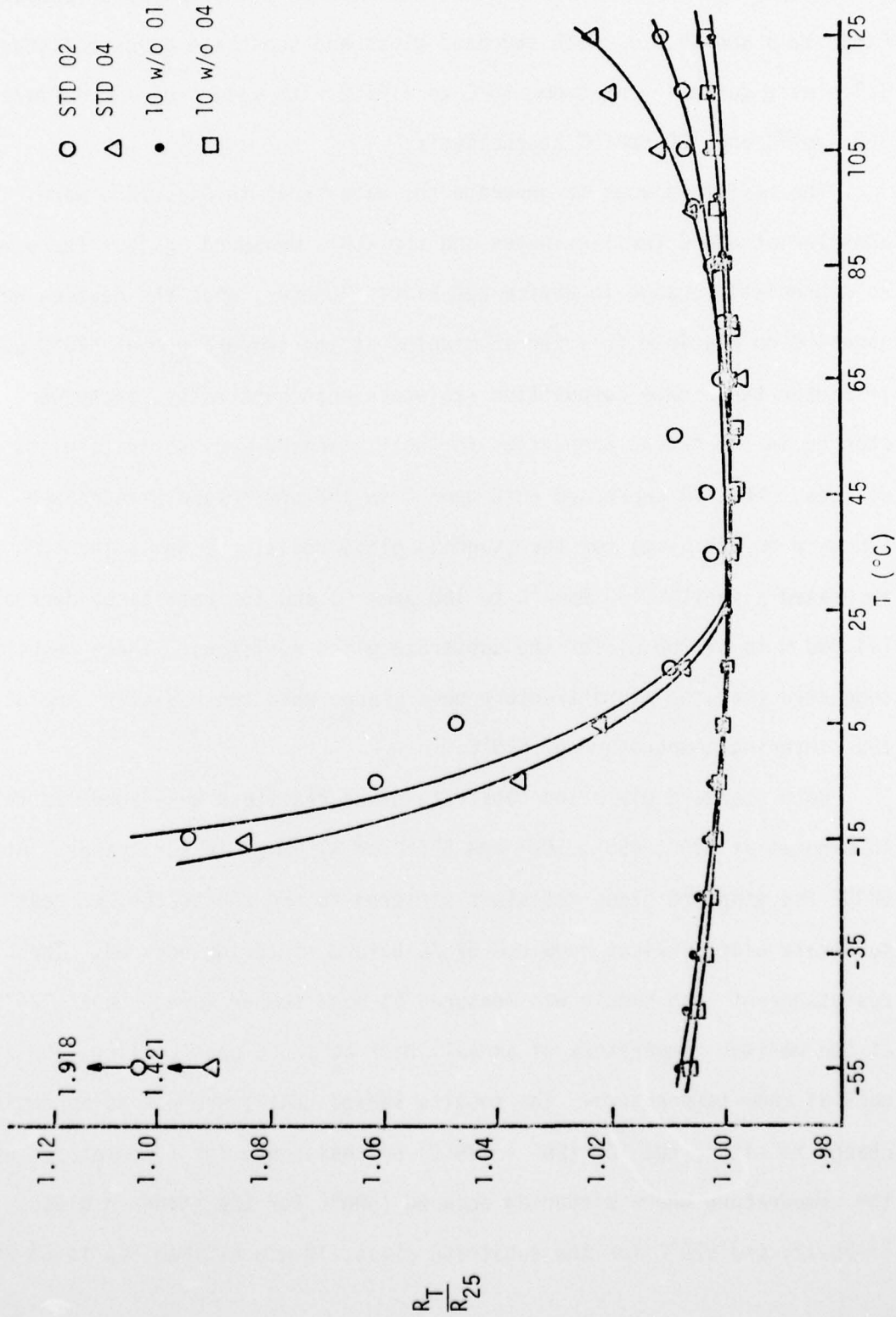


Figure IV.3 Effect of 10 w/o AlSiMag 614 in 63-25-12 Glass on 5 w/o RuC<sub>2</sub> Resistors Sintered on AlSiMag 614 Substrate - TCR.

non-supported resistors made using glasses with and without dissolved substrate are shown in Fig. IV.4. The TCR's of these resistors were quite different from the resistors sintered to AlSiMag 614 substrates (compare Figs. IV.3 and IV.4.) Both standard glass and substrate glass resistors TCR's were quite linear from  $-55^{\circ}\text{C}$  to  $+125^{\circ}\text{C}$  with values of approximately  $340\text{ ppm}/^{\circ}\text{C}$  and  $120\text{ ppm}/^{\circ}\text{C}$  respectively.

The resistors used to generate the data shown in Fig. IV.4 were annealed at  $420^{\circ}\text{C}$  for 12 minutes and the TCR's measured again. There was no appreciable change in device behavior. However, when the devices were annealed on platinum foil for 15 minutes at the temperature of  $520^{\circ}\text{C}$  used to sinter these same composition resistors onto substrates, there were changes in electrical properties for both standard and substrate glass devices. The TCR decreased ( $340\text{ ppm}/^{\circ}\text{C}$  to  $180\text{ ppm}/^{\circ}\text{C}$ ) and  $\rho$  increased ( $25\ \Omega\text{-cm}$  to  $400\ \Omega\text{-cm}$ ) for the standard glass resistors, while the TCR increased slightly ( $150\text{ ppm}/^{\circ}\text{C}$  to  $180\text{ ppm}/^{\circ}\text{C}$ ) and the resistance decreased ( $14,000\ \Omega$  to  $11,000\ \Omega$ ), for the substrate glass resistors. These results suggested that the microstructure does change when the resistors are at the sintering temperature of  $520^{\circ}\text{C}$ .

Both standard glass and substrate glass resistors were annealed for 15 minutes at  $425^{\circ}$ ,  $450^{\circ}$ ,  $500^{\circ}$  and  $525^{\circ}\text{C}$  on AlSiMag 614 substrates. At  $500^{\circ}\text{C}$  the standard glass resistors sintered to the substrates, whereas the substrate glass devices required  $525^{\circ}\text{C}$  before sintering occurred. The resistance of each sample was measured at room temperature then at  $125^{\circ}\text{C}$ , at the maximum temperature of anneal, back at  $125^{\circ}\text{C}$  upon cooling, and finally back at room temperature. The results showed that there was no appreciable change in either hot TCR ( $25^{\circ}$  -  $125^{\circ}\text{C}$ ) or resistance for temperatures up to the temperature where sintering occurred ( $500^{\circ}\text{C}$  for the standard glass, 63-25-12, and  $525^{\circ}\text{C}$  for the substrate glass, 10 w/o AlSiMag 614 in 63-25-12).

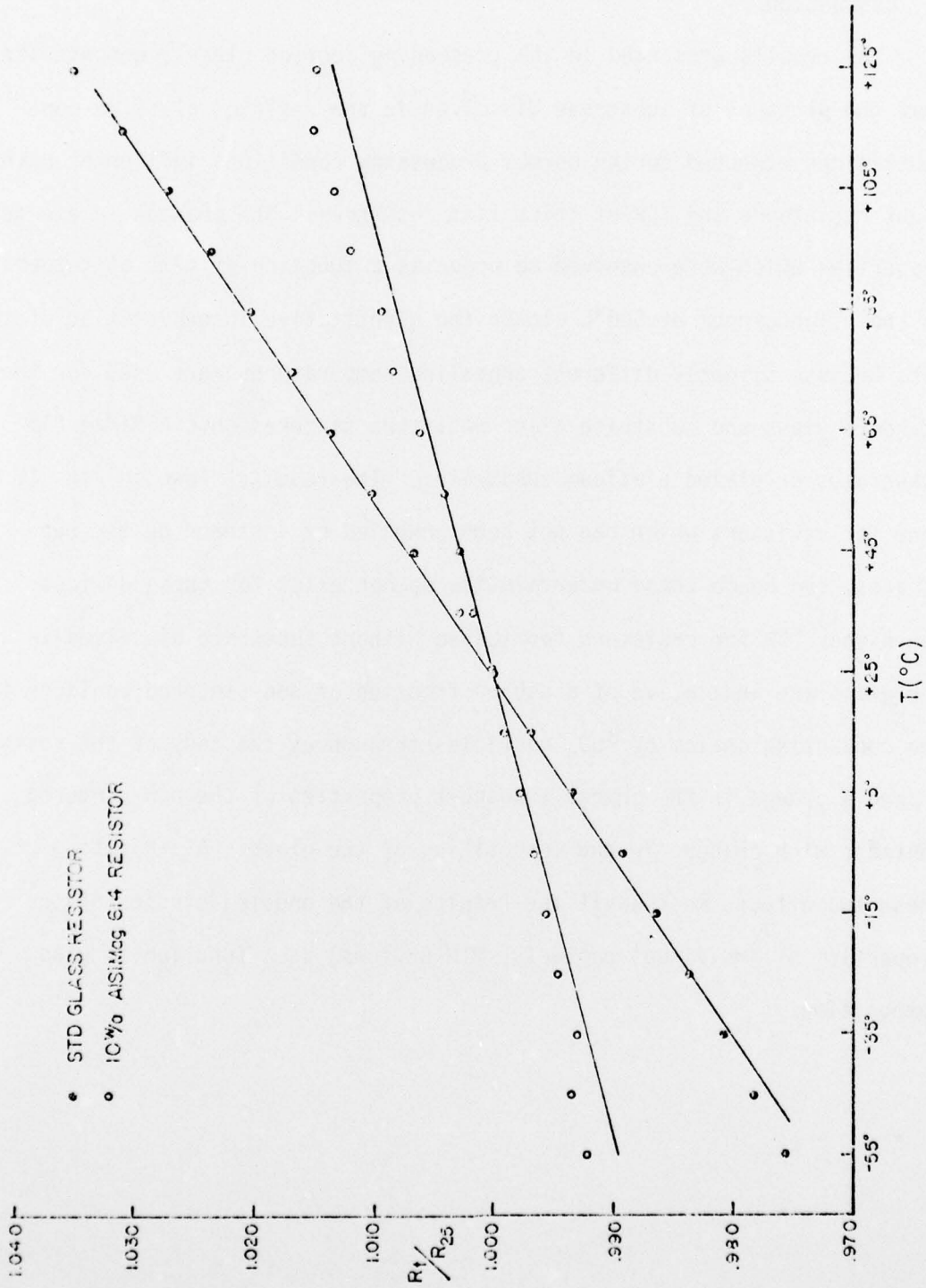


Figure IV.4 Effect of 10 w/o AISiMag 614 in 63-25-12 Glass on Non-supported 5 w/o RuO<sub>2</sub> Resistors - TCR

At the sintering temperature, the room temperature resistance before and after the anneal changed from 30-50%.

### C. DISCUSSION

The results presented in the preceding section clearly demonstrate that the presence of substrate dissolved in the resistor glass in concentrations expected during normal processing conditions influences both sheet resistance and TCR of thick film resistors. The changes in electrical properties which were observed to occur as a function of time at temperatures in the neighborhood of 500°C clouds the quantitative interpretation of the data because slightly different annealing temperatures were used for the standard glass and substrate glass resistors sintered onto AlSiMag 614 substrates or glazed platinum substrates. The results shown in Fig. IV.4 were for resistors which had not been annealed or sintered on the substrates, and hence these uncertainties do not exist for these devices. The higher TCR for resistors fabricated without substrate dissolved in the glass are indicative of a higher fraction of non-sintered contacts in the conducting chains of  $\text{RuO}_2$  particles throughout the body of the resistor, or/and a change in the charge transport properties of the non-sintered contacts with changes in the composition of the glass. A separation of these two effects must await the results of the ongoing studies of the properties of individual contacts (MIM devices) as a function of glass composition.

## V. FUTURE PLANS

The kinetics of Ostwald ripening of  $\text{RuO}_2$  in the glass will be determined by X-ray diffraction line broadening and surface area measurements as a function of glass composition, and the kinetics of the initial stage of liquid phase sintering of  $\text{RuO}_2$  will be calculated from these data. These results will then be correlated utilizing the previously developed model for microstructure development, and the influence of glass composition established. The equilibrium solubility of  $\text{RuO}_2$  in glass will be measured as a function of glass composition and temperature in order to calculate the sintering kinetics of  $\text{RuO}_2$  from measurements of ripening kinetics. The effects of substrate dissolution on charge transport processes important in non-sintered contacts will be determined by fabricating metal-insulator-metal (MIM) structures and measuring the dielectric properties, bulk resistivity and break down characteristics of the glass, as well as the current-voltage characteristics of the MIM all as a function of glass composition. The dependence of both the glass properties and the electrical properties of the non-sintered contacts on glass composition will be incorporated into a revised charge transport model for thick film resistors.

VI. REFERENCES

1. L. Hailes and W. A. Crossland, "Thick Films: Substrate-Conductor Relationship," *Electronic Pack. and Prod. (Int.)*, 3-7, July, 1972.
2. W. A. Crossland and L. Hailes, "Thick Film Conductor Adhesion", *S. State Tech.*, 14, 42-47 (1971).
3. R. W. Vest, "Conduction Mechanisms in Thick Film Microcircuits," Final Technical Report, Purdue Research Foundation Grant Nos. DAHC - 15-70-G7 and DAHC - 15-73-G8, ARPA Order No. 1642, December 1975.
4. R. W. Vest, "The Effects of Substrate Composition on Thick Film Circuit Reliability," Final Technical Report on Contract No. N00019-76-C-0354, 28 February 1977.
5. R. L. Reed and L. R. Barrett, "The Slagging of Refractories; II. The Kinetics of Corrosion," *Trans. Brit. Ceram. Soc.*, 63, 509-534 (1964).
6. A. K. Cooper, Jr., "Effects of Moving Boundary on Molecular Diffusion Controlled Dissolution or Growth Kinetics," *Trans. Faraday Soc.* 58, 2468-72 (1962).
7. A. R. Cooper, Jr., and W. D. Kingery, "Dissolution in Ceramic Systems: I, Molecular Diffusion, Natural Convection, and Forced Convection Studies of Sapphire Dissolution in Calcium Aluminum Silicate," *J. Amer. Ceram. Soc.*, 47, 37-43 (1964).
8. B. G. Levich, "Theory of Concentration Polarization", *Discussions Faraday Soc.*, 1, 37-43 (1947).
9. D. P. Gregory and A. C. Riddiford, "Transport to Surface of a Rotating Disc," *J. Chem. Soc.*, pp. 3756-64 (1956).
10. R. L. Reed and L. R. Barrett, "The Slagging of Refractories; Part I The Controlling Mechanism in Refractory Corrosion," *Trans. Brit. Ceram. Soc.*, 63, 671-676 (1964).
11. N. McCallum and L. R. Barrett, "Some Aspects of the Corrosion of Refractories," *Trans. Brit. Ceram. Soc.*, 51, 523-548 (1952).
12. B. N. Samaddar, W. D. Kingery, and A. R. Cooper, Jr., "Dissolution in Ceramic Systems: II, Dissolution of Alumina, Mullite, Anorthite, and Silica in Calcium Aluminum Silicate Slag," *J. Amer. Ceram. Soc.*, 47, 249-254 (1964).
13. A. N. Ryabov, T. I. Kiseleva, and L. B. Kulikova, "Rate of Dissolution of Aluminum Oxide in Molten Potassium Bisulfate," *ZH Prik Khim*, 48, 407-48 (1975).
14. M. Truhlarova, "Dissolution of  $\text{SiO}_2$  and  $\text{Al}_2\text{O}_3$  in Four Basic Glass Melts at Viscosity  $\log \eta = 2.5$ ," *Silikaty*, 18, 31-43, (1974).

15. M. Safdar, G. H. Frischat, and H. W. Hermicke, "Korrosion von Aluminiumoxid durch Vanadiumpentoxid Schmelzen," Ber. Dt. Keram. Ges., 51, 291-294 (1974)
16. P. F. Becher and J. S. Murday, J. Mat. Sci., 12, 1088-1094 (1977).
17. J. Frenkel, "Viscous Flow of Crystalline Bodies under the Action of Surface Tension", J. Phys. (U.S.S.R.), 9, 385 (1945).
18. G. C. Kuczynski B. Neuville and H. P. Tower, "Study of Sintering of Poly (Methyl Methacrylate)", J. Appl. Polymer Sci., 14, 2069 (1970).
19. I. B. Cutler, "Effect of Water Vapor on Sintering of Glass Powder Compacts," J. Am. Ceram. Soc., 52 [1], 11-13 (1969).
20. H. Scnolye, "Gasses and Water in Glass: I, "Glass Ind., 47 [10], 546-51 (1966); "II," ibid [11], 622-28; "III," ibid [12], 670-75.
21. N. M. Parikh, "Effect of Atmosphere on Surface Tension of Glass," J. Am. Ceram. Soc., 41 [1], 18-22 (1958).

APPENDIX  
GLASS PREPARATION

A consideration of the phase diagram for the  $\text{PbO-B}_2\text{O}_3\text{-SiO}_2$  system [A1, A2] reveals that the 63-25-12 composition lies only a few weight percent on the lead rich side of a two liquid phase region, and the later phase diagram work [A2] on this system puts the composition at the boundary of a metastable region. The 70-20-10 composition is slightly removed from the metastable region toward the PbO corner of the diagram. When attempting to fabricate either of these glass compositions by heating appropriate quantities of the mixed constituent oxides, it was discovered that two liquid phases always formed and that it was very difficult to obtain a homogenous glass melt due to large differences in densities of the two liquid phases. For this reason, a special furnace was designed and constructed so that the glass melts could be stirred at temperature in order to speed the homogenization. The furnace, shown schematically in Fig. A1, was maintained at a constant temperature by use of a Barber Coleman 540 Series solid state controller operating from a chromel-alumel control thermocouple. The glass melts were contained in a 75 ml platinum crucible secured in a hollowed out cavity in an alumina refractory brick. The crucible assembly could be lowered quickly out of the furnace so that the melt could be fritted or poured into a mold as required.

Frits of the 63-25-12 and 70-20-10 base glasses were prepared by mixing appropriate quantities of  $\text{Pb}_3\text{O}_4$ ,  $\text{H}_3\text{BO}_3$ , and  $\text{SiO}_2$  in a rolling jar, stirred in the furnace at  $950^\circ\text{C}$  for 90 minutes to produce a homogeneous melt, and fritted in deionized water. Glasses containing varying amounts of substrate were prepared by combining appropriate amounts of the 70-20-10 or 63-25-12 frits with pieces of AlSiMag 614 substrates, grinding the mixtures to -80

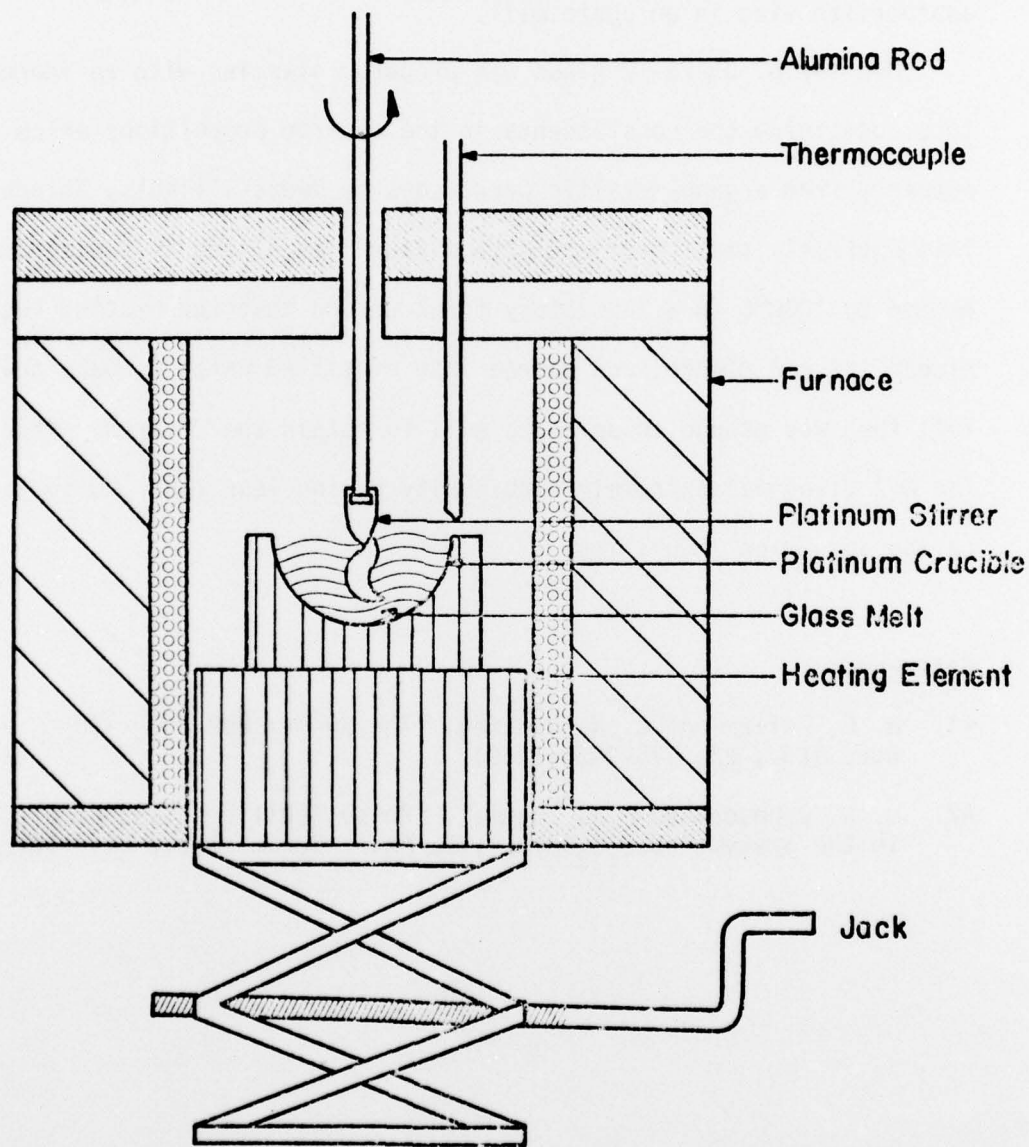


Figure A.1 Glass Melting Furnace

mesh, and melting at 1050°C in the glass furnace under agitation for 90 minutes. The melts were then fritted in deionized water and ground to the appropriate size in an agate mill.

One lot of 63-25-12 glass was prepared starting with an inorganic mixture containing the constituents in the desired proportions which had been prepared from organo-metallic precursors by Owens-Illinois, Toledo, Ohio. This extremely small particle size mixture was placed in a platinum crucible and heated to 1000°C in a laboratory furnace such that the heating rate did not exceed 1°C per minute, and poured into distilled water to make the frit. The frit then was ground in an agate mill to obtain the desired particle size. The O-I glass was extremely high purity having less than 200 ppm combined cation and anion impurities.

#### References

- A1. R. F. Geller and E. N. Bunting, "The System PbO-B<sub>2</sub>O<sub>3</sub>-SiO<sub>2</sub>", J. Res. Natl. Bur. Std., 23, 275-283 (1939).
- A2. D. W. Johnson and F. A. Hummel, "Phase Equilibria and Liquid Immiscibility in the System PbO-B<sub>2</sub>O<sub>3</sub>-SiO<sub>2</sub>", J. Amer. Ceram. Soc., 51, 196-201 (1968).